



Measuring the propagation of financial distress with Granger-causality tail risk networks[☆]

Fulvio Corsi^{a,b}, Fabrizio Lillo^c, Davide Pirino^{d,*}, Luca Trapin^e

^a University of Pisa, Italy

^b City University London, United Kingdom

^c University of Bologna, Italy

^d University of Rome Tor Vergata and Scuola Normale Superiore, Pisa, Italy

^e Catholic University of Sacred Heart, Milano, Italy



ARTICLE INFO

Article history:

Received 12 January 2018

Received in revised form 25 June 2018

Accepted 27 June 2018

Available online 18 July 2018

JEL classification:

G00

G01

G21

H63

C12

Keywords:

Financial stability

Systemic risk propagation

Granger-causality

Sovereign debt crisis

Illiquidity

Flight-to-quality

ABSTRACT

Using the test of Granger-causality in tail of Hong et al. (2009), we define and construct Granger-causality tail risk networks between 33 systemically important banks (G-SIBs) and 36 sovereign bonds worldwide. Our purpose is to exploit the structure of the Granger-causality tail risk networks to identify periods of distress in financial markets and possible channels of systemic risk propagation. Combining measures of connectedness of these networks with the ratings of the sovereign bonds, we propose a flight-to-quality indicator to identify periods of turbulence in the market. Our measure clearly peaks at the onset of the European sovereign debt crisis, signaling the instability of the financial system. Finally, we use the connectedness measures of the networks to forecast the quality of sovereign bonds. We find that connectedness is a significant predictor of the cross-section of bond quality.

© 2018 The Authors. Published by Elsevier B.V. This is an open access article under the CC BY-NC-ND license (<http://creativecommons.org/licenses/by-nc-nd/4.0/>).

1. Introduction

The surge of market distress and the rapid spread of uncertainty may lead a significant number of market players to rethink their priorities and investment strategies triggering a rebalancing of their portfolios (Caballero and Krishnamurthy, 2008). When investors have similar portfolios, coordinated rebalancing might lead to massive sales of risky assets (Cont and Wagalath, 2013, 2016; Corsi

et al., 2016) and purchases of safer ones. These episodes are known as “flight-to-quality” and can play a prominent role in the propagation and deepening of financial crises. The ability of identifying and possibly anticipating such phenomena is of great importance in the context of early-warning and monitoring of systemic risk (Demirgüç-Kunt and Detragiache, 1998; Kaminsky and Reinhart, 1999; Harrington, 2009; Scheffer et al., 2009, 2012; Barrell et al., 2010; Duttagupta and Cashin, 2011; Kritzman et al., 2011; Allen et al., 2012; Arnold et al., 2012; Bisias et al., 2012; Merton et al., 2013; Oet et al., 2013).

The literature on the identification and characterization of flight-to-quality episodes has followed two main streams. The first one, followed for example by Beber et al. (2009), investigates proprietary data on order flow looking for direct evidences of flight-to-quality episodes. The second one exploits publicly available price data, and uses econometric tools to identify periods of flight-to-quality (Baur and Lucey, 2009; Dovern and van Roye, 2014; Greenwood et al., 2015; Adrian and Brunnermeier,

[☆] This work is supported by the European Community H2020 Program under the scheme INFRAIA-1-2014-2015: Research Infrastructures, grant agreement #654024, SoBigData: Social Mining and Big Data Ecosystem (<http://www.sobigdata.eu>). We thank Flavia Barsotti, Umberto Cherubini, Piero Mazzarisi and Aldo Nassigh for useful comments and discussions, and Andrea Basile and Andrea Sillari for providing the data.

* Corresponding author.

E-mail addresses: fulvio.corsi@unipi.it (F. Corsi), fabrizio.lillo@unibo.it (F. Lillo), davide.pirino@gmail.com (D. Pirino), luca.trapin@unicatt.it (L. Trapin).

2016; Brownlees and Engle, 2016). The method we propose in this paper belongs to the second class and constructs Granger-causality tail risk networks using the idea of Granger-causality in tail of Hong et al. (2009). We apply our approach to identify flight-to-quality from systemically important banks (G-SIBs) toward sovereign bonds worldwide.

Sovereign debt securities form a considerable fraction of banks' total assets and since big market players are usually levered institutions pursuing a pro-cyclical leverage¹ strategy (Adrian and Shin, 2010, 2014; Greenwood et al., 2015), periods of financial distress can be triggered by banks massively selling their assets to recover their optimal leverage level after a shock. Moreover, the micro-prudential regulation requires financial institutions to adjust their capital depending on the level of risk of their portfolio. As banks are subject to risk-based capital ratio constraints, they may be also forced to rebalance their portfolios toward safer assets to comply with the regulation (Cifuentes et al., 2005; Braouezec and Wagalath, 2016). Following these arguments, we expect that a flight-to-quality episode has good chance to be identified in the bank-sovereign bond system. Within this system, we should observe two reinforcing effects in times of distress. First, investors selling banks' stocks and "bad" sovereign bonds, while performing massive purchases of "good" bonds. Second, distressed banks pursuing a de-leveraging strategy or complying with the regulatory constraint selling low-rated bond holdings. Hence, due to market impact and assets' illiquidity, large movements of bond prices (and hence of bond yields) are expected as a consequence of large equity drops of banks.

In order to econometrically identify this chain of events from market prices, we propose to use the Granger-causality test in tail of Hong et al. (2009), which allows to test if the occurrence of a left or right tail event of a random variable is systematically followed (in a statistical sense) by the occurrence of a left or right tail event of a second random variable. We study the causal relationships in tail between 33 systemically important banks² and 36 sovereign bonds and cast this information in bank-bond bipartite networks³ where the link between a bank and a bond indicates the existence of Granger-causality in tail. We define measures of connectedness for the Granger-causality tail risk networks that have a simple economic interpretation as indicators of fire-sales and fire-buys, under the assumption that the fundamentals of the analyzed assets do not change over the considered period. Combining these measures with Standard & Poor's (S&P) ratings, we can thus identify periods of simultaneous "bad" bond fire-sales and "good" bond fire-buys.⁴ This double effect corresponds to a natural characterization of flight-to-quality, where the general distrust pushes investors toward low-risk assets, by freeing resources from high-risk ones.

Finally, we investigate the ability of our network connectedness measures of forecasting the future quality rankings of the sovereign bonds. We define four time-varying bond quality measures based on the correlation between CDS spreads and the bond yields, the bond yield volatility, and the yield spreads,⁵ and test the out-of-sample forecasting performances of our connectedness measures. Most importantly, the four quality measures are all market-based proxies of the sovereign debts quality, and so they can provide

insightful information to surveillance authorities. We find that during periods of distress, the connectedness of the Granger-causality tail risk networks is a significant predictor of the ranking of the bond quality measures.

Our work contributes to several strands of literature. Concerning flight-to-quality, the analysis by Beber et al. (2009) sheds insightful light on how liquidity and quality are chased in the market. Unusual capital flows are used in Beber et al. (2009) to proxy flights, both to liquidity and to quality. However this kind of data are unavailable, partial, or very difficult to collect. Defining an econometric measure of flight-to-quality based on easily available daily market prices, considerably reduces the data requirements in our approach. This allows us to considerably extend the time span of our analysis compared to the one in Beber et al. (2009), considering the equity and bond market developments from the beginning of 2006 to February 2014. As a consequence, our analysis profits from the presence of two important periods of financial distress. In exchange, we pay a price in terms of interpretation of our results. As we do not directly observe trading activity, we cannot distinguish between a bank reacting to a large drop of its equity value with a flight-to-quality on the sovereign debt market, and a similar flight-to-quality operated by a large institutional investor liquidating bank stocks. In both cases there will be unexpected variation of the sovereign bond yields as a consequence of large equity drops of the banks involved. As anticipated above, we operate under the assumption that the assets' fundamentals are stable over the period, and interpret the extreme market movements as if they were fully generated by price-mediated contagion. Our analysis is thus representative of a worst case scenario flight-to-quality. Nonetheless, we uncover interesting aspects of the flight-to-quality dynamics that are relevant from a systemic risk management perspective and for regulators. Complementing the results of Beber et al. (2009), we document that investors, do chase for quality during financial crises, but they do it in different ways: in some cases, such as during and after the Lehman crisis, they simply chase quality by buying sovereign debt of any type, while in others, such as during the European sovereign debt crisis, they require only top-quality sovereign debt, i.e. the flight-to-quality occurs exclusively toward AAA-rated sovereign bonds.

Another flight-to-quality paper related to ours is Baur and Lucey (2009). Here the authors define [...] *flight-to-quality from stocks to bonds as a significant decrease in the correlation coefficient in a (stock market) crisis period compared to a benchmark period resulting in a negative correlation level*. In summary Baur and Lucey (2009) look for significant negative changes of the bond-stock correlation that result in a change of the sign of the correlation from positive to negative, or from negative to even more negative. The rationale is that flight-to-quality is identified by stocks and bonds moving in opposite directions, hence it is not enough that the correlation decreases, it must turn into a negative value. The econometric tools presented in our paper share with Baur and Lucey (2009) the appealing feature of being based on easily accessible data but substantially differs from it along two lines. First, instead of looking to significant changes of correlations, we put the focus on significant causality links between extreme variations of stocks (of large banks) and extreme variations of bond yields (of the sovereign type). Second, while in Baur and Lucey (2009) periods of crises are inputted in the model via a dummy variable and thus are identified *ab initio*, in our approach we backtest that the risk measures do in fact peak around crises, hence reinforcing their role as indicators of financial distress. We also contribute to the literature on financial distress. In particular, our work is related to the paper by Dovern and van Roye (2014). Here the authors define a country-specific index of financial stress without explicitly adopting a network approach. In fact, a factor model is used in order to extract, from a country-specific basket of stationary and standardized indicators of financial stress,

¹ In periods of extraordinary distress and uncertainty, de-leveraging is a common strategy also for financial institution not actively managing their leverage, see Chen et al. (2014).

² In particular, we rely on the definition of G-SIBs defined by Basel III regulatory framework. For more detail, see <http://www.bis.org/bcb/basel3.htm>.

³ A bipartite network is a graph whose vertices can be divided into two disjoint sets such that every edge connects a vertex in one set to one in the other set.

⁴ The precise definition of bad and good bonds will be clarified later.

⁵ Yield spreads are defined as the difference between a government bond yield and the German bond yield at the same maturity.

a common component which is used as unique indicator of financial stress for that country. Transmission of stress is then captured via a GVAR model (Pesaran et al., 2009). Our philosophy shares with that of [Dovern and van Roye \(2014\)](#) the idea of defining indicators of financial distress via an econometric approach that takes fully into consideration data heteroskedasticity, hence removing bias induced by sudden variations of the volatility regime of the assets involved. Nevertheless, there is a striking difference since our approach focuses on tail events and, for this reason, is designed to analyze propagation of financial distress.

Finally, we relate to the literature on Granger-causality networks. These have been introduced in systemic risk studies by [Billio et al. \(2012\)](#) to identify and quantify periods of financial turbulence, characterized by abnormal levels of Granger inter-connectedness among equities of hedge funds, banks, broker/dealers, and insurance companies. Our paper, although being inspired by the analysis of [Billio et al. \(2012\)](#), moves away from it in at least two respects: first, we adopt a bipartite network of equities and bonds, a choice dictated by the will of investigating the effect of crises on sovereign debt and, second, we adopt the Granger-causality test in the tail by [Hong et al. \(2009\)](#), since we believe that it is suited to describe events pertaining to a crisis.

The paper is organized as follows: Section 2 presents the test of Granger-causality in tail of [Hong et al. \(2009\)](#) and explains the construction of a Granger-causality tail risk network. Section 3 gives the detail of the investigated dataset. Section 4 describes the structure of the bank-bond Granger-causality tail risk networks. Section 5 presents and discusses our flight-to-quality indicator. Section 6 describes the out-of-sample forecasts of the bond quality based on the connectedness of the Granger-causality tail risk networks. Section 7 concludes. Technical details are relegated to the Appendix.

2. Constructing a Granger-causality tail risk network

To construct a bank-bond Granger-causality tail risk network, we rely on an econometric approach that only requires time series of banks' equity returns⁶ and sovereign bond yields. This has the advantage of being implementable at any frequency (weekly, daily or even higher, depending on the availability of data) without requiring any not publicly available dataset, such as order flow data, which are notoriously very hard to obtain.

We define a bank-bond Granger-causality tail risk network as a bipartite network where banks and bonds form the two sets of nodes, and the existence of a bank-bond edge is established with the test of Granger-causality in tail of [Hong et al. \(2009\)](#). Rejection of the null hypothesis of the test provides statistical support for a causal relationship in the tail between a bank and a bond, and an edge is created. Depending on the direction of causality (bank \rightarrow bond) and the side of the tail (upper or lower), eight Granger-causality tail risk networks can be investigated.

The Granger-causality test in tail of [Hong et al. \(2009\)](#) is the econometric tool at the core of the network construction. Consider two time series $\{Y_{1,t}\}_{t=1}^T$ and $\{Y_{2,t}\}_{t=1}^T$, such as bond yield variations and equity log-returns, and suppose to test whether extreme events in the lower tail of $Y_{2,t}$ Granger-cause extreme events in the lower tail⁷ of $Y_{1,t}$. The first step of the procedure is to identify which are the extreme events in the history of both series.

For this purpose, following the approach of [Hong et al. \(2009\)](#), we estimate a parametric model for the conditional (on past history) Value-At-Risk (VaR) of $\{Y_{1,t}\}_{t=1}^T$ and $\{Y_{2,t}\}_{t=1}^T$. For the parametric model, as well as the numerical routines, we borrow from the popular CAViaR approach developed by [Engle and Manganelli \(2004\)](#). This class of models fully satisfies the assumptions required for the application of the [Hong et al. \(2009\)](#) test. For more details about the VaR model and the corresponding parameter estimates we refer to [Appendix A](#). The outcome of the [Engle and Manganelli \(2004\)](#) procedure is a parametric estimate of the conditional VaR series $\{V_{i,t}^{(\alpha)}\}_{t=1}^T$ defined in the standard fashion

$$\text{Prob} \left[Y_{i,t} \leq -V_{i,t}^{(\alpha)} \mid F_{t-1} \right] = \alpha, \quad i = 1, 2,$$

where F_t denotes the information available at time t and α defines the probability level. In the empirical analysis, we choose $\alpha = 10\%$ as a trade-off between the necessity of focusing on extreme events and that of having a sufficiently high number of observations.⁸ Once the two conditional VaR series have been estimated we can apply the one-way Granger-causality test by [Hong et al. \(2009\)](#). Define the series of hits as⁹ $\{Z_{1,t}\}_{t=1}^T$ and $\{Z_{2,t}\}_{t=1}^T$, with $Z_{i,t} \equiv \mathbb{1}_{\{Y_{i,t} < -V_{i,t}^{(\alpha)}\}}$, the test compares the null

$$\mathbb{H}_1^0 : \mathbb{E} \left[Z_{1,t} \mid \{Y_{1,t-k}\}_{k=1}^{t-1} \right] = \mathbb{E} \left[Z_{1,t} \mid \{Y_{1,t-k}, Y_{2,t-k}\}_{k=1}^{t-1} \right] \quad (1)$$

against the alternative

$$\mathbb{H}_1^A : \mathbb{E} \left[Z_{1,t} \mid \{Y_{1,t-k}\}_{k=1}^{t-1} \right] \neq \mathbb{E} \left[Z_{1,t} \mid \{Y_{1,t-k}, Y_{2,t-k}\}_{k=1}^{t-1} \right]. \quad (2)$$

The interpretation of \mathbb{H}_1^0 and \mathbb{H}_1^A is straightforward. If the null hypothesis is rejected it means that the occurrence of a large event in $Y_{2,t}$ has significantly impacted the probability of a future occurrence of an extraordinary event in $Y_{1,t}$, and we say that $Y_{2,t}$ Granger-cause $Y_{1,t}$ in the tail. The rejection of the null, hence the creation of the bank-bond link in the network, occurs if and only if for several times in the time interval considered an extreme negative log-return of the bank equity is followed by an extreme negative variation of the bond yield.

Note that the conditioning information includes at most instant $t-1$, while the conditioned event $\{Y_{1,t} < -V_{1,t}^{(\alpha)}\}$ is occurring at t , whence the genuine causality of the approach. We pay particular care in the construction of both the VaR measure and the Granger-causality test to fully preserve causality using, at any point in time, only past information. [Appendix A](#) describes in detail the solution adopted.

Let $\hat{\rho}(j)$ be the sample cross-correlation function between $\{Z_{1,t}\}_{t=1}^T$ and $\{Z_{2,t}\}_{t=1}^T$ at positive lag j , i.e.

$$\hat{\rho}(j) = \frac{\hat{C}(j)}{S_1 S_2},$$

⁸ Results with other choices of α are available upon request.

⁹ We indicate with $\mathbb{1}_{\{A\}}$ the indicator function of the event A , that is for all ω in the probability space Ω

$$\mathbb{1}_{\{A\}}(\omega) = \begin{cases} 1 & \text{if } \omega \in A \\ 0 & \text{if } \omega \notin A. \end{cases}$$

⁶ We could, in principle, extend the analysis to other types of stocks or indexes. Our results show, however, that focusing on the bank-bond system is largely sufficient to identify crises and flight-to-quality phenomena, so for conciseness we do not consider stocks different from banks' equities and we restrict the analysis to this minimal data requirement.

⁷ Equivalent procedures apply when testing for Granger-causalities in the other tails or reversed causality.

where $S_i^2 = \alpha_i (1 - \alpha_i)$ and $\hat{C}(j) = T^{-1} \sum_{t=1+j}^T (Z_{1,t} - \alpha_1) (Z_{2,t-j} - \alpha_2)$, with $j = \{1, 2, \dots, T-1\}$ and $\alpha_i = T^{-1} \sum_{t=1}^T Z_{i,t}$. Hong et al. (2009) show that, under \mathbb{H}_1^0

$$Q_1(M) = \frac{T \sum_{j=1}^{T-1} k\left(\frac{j}{M}\right)^2 \hat{\rho}(j)^2 - C_{1,T}(M)}{D_{1,T}(M)^{\frac{1}{2}}} \xrightarrow{D} N(0, 1)$$

when both the number of observations $T \rightarrow \infty$ and the bandwidth $M = cT^\nu \rightarrow \infty$ ($c > 0$, $0 < \nu < \frac{1}{2}$), where $k(x)$ is a suitable kernel function,¹⁰ and $C_{1,T}(M)$ and $D_{1,T}$ are known constants. Note that $\hat{C}(j)$ considers only positive values of the lag j , i.e. lagged correlation between past observations of $Z_{2,t}$ and future observations of $Z_{1,t}$ (since we are testing the causal relation of the second variable on the first one). Under \mathbb{H}_1^A it is

$$\frac{M^{1/2}}{T} Q_1(M) \xrightarrow{p} \frac{1}{\left(2 \int_0^\infty k(z)^4 dz\right)^{\frac{1}{2}}} \sum_{j=1}^\infty \hat{\rho}(j)^2,$$

which implies that the test has asymptotic unit power at any confidence level. If $Q_1(M) > c_\beta$, where c_β is the β -quantile of a Normal distribution function with zero mean and unit standard deviation, then we say that $\{Y_{2,t}\}_{t=1}^T$ Granger-causes the series $\{Y_{1,t}\}_{t=1}^T$ in the tail. Throughout the analysis we choose $\beta = 95\%$ and hence $c_\beta = 1.6449$. Moreover, following the small-sample properties of the test as reported by Hong et al. (2009), we set $M = 5$ for the value of the bandwidth parameter.

For completeness and in order to compare our results with those of Billio et al. (2012), we also construct a bank-bond network where connections are established with the standard Granger (1969) causality test. Differently from Hong et al. (2009), Granger (1969) tests for causality in the conditional mean of $Y_{1,t}$ and $Y_{2,t}$, i.e. it tests the null hypothesis

$$\mathbb{H}_G^0 : \mathbb{E} \left[Y_{1,t} | \{Y_{1,t-k}\}_{k=1}^{t-1} \right] = \mathbb{E} \left[Y_{1,t} | \{Y_{1,t-k}, Y_{2,t-k}\}_{k=1}^{t-1} \right] \quad (3)$$

against the alternative

$$\mathbb{H}_G^A : \mathbb{E} \left[Y_{1,t} | \{Y_{1,t-k}\}_{k=1}^{t-1} \right] \neq \mathbb{E} \left[Y_{1,t} | \{Y_{1,t-k}, Y_{2,t-k}\}_{k=1}^{t-1} \right]. \quad (4)$$

The main difference between the couple of null-alternative hypotheses in (3) and (4) and those in (1) and (2) is the substitution of the series $Y_{i,t}$ with $Z_{i,t}$, which signals the presence of tail events. Therefore, when \mathbb{H}_G^0 is rejected we say that $Y_{2,t}$ Granger-cause $Y_{1,t}$ in the mean. Details on the construction of this network can be found in Appendix C.

3. The dataset

Our dataset is composed of $j = 1, \dots, 33$ equities of globally important banks (G-SIBs) defined by Basel III regulatory framework and $i = 1, \dots, 36$ sovereign debt bonds (with a maturity of 5 years) of different countries in America, Europe and Asia. We indicate with $\gamma_{i,t}$ the nominal 5-years maturity bond yield of country i at day t . All the time series of bonds and equities end on February, 14, 2014, but they start at different dates. Equities are mostly available by the end of the nineties, while bonds become available after the beginning of 2000. For each country i we have also at our disposal the daily time series of five-years maturity CDS spread, a quantity that we indicate as $S_{i,t}$ henceforth. Most of the CDS spread time series end on January, 13, 2014 and are available since early 2000s. Detailed information, along with Tables

with summary statistics, on the three blocks of data are provided in Appendix B.

Finally, we mention that in Section 6.1, in order to properly define the quality measures based on the correlation between CDS spreads and bond yields, we require a proxy for the risk-free interest rate r . For each bond, depending on the currency, we use the zero-coupon curve of the corresponding maturity and currency derived by a bootstrapping procedure.¹¹

4. The bank-bond Granger-causality tail risk networks

Since our interest is exploring financial distress identifying flight-to-quality episodes in the bank-bond system, we mainly focus our analysis on the causal relationship between the left tail (losses) of the bank equity distribution and both the left and right tails of the bond yield distribution. Under the assumption of stable fundamentals, causal shocks between the tails can be economically interpreted as fully generated by price-mediated contagion. In particular, a negative shock to the equity of bank j causing large negative yield variations to the bond of country i can be interpreted as a bond appreciation due to massive purchases, or fire-buy. A negative shock to a bank equity suddenly increasing the bond yield of a country can be interpreted as a fire-sale on the corresponding sovereign debt inducing a strong depreciation. Both mechanisms can be induced by either a large institutional investor liquidating risky assets (banks' stocks and low-rated sovereign bonds) and buying sovereign debts of countries with strong fiscal discipline, or the management of a bank experiencing an equity drop that reacts selling the risky bonds in its balance sheet, while simultaneously purchasing high quality bonds, to re-equilibrate the regulatory risk-based capital ratio above the minimum level established by the regulator.

Our identification of fire-sales and fire-buys is based on an econometric analysis of equity returns and bond yield variations rather than balance sheet data. Therefore, we can only argue that a distressed sale or distressed buy occurs in a statistical sense. For this reason, we establish the existence of a *statistical* fire-sale (*statistical* fire-buy) between bank j and bond i when the Hong et al. (2009) test supports a causal relationship between the lower tail of the bank and the upper (lower) tail of the bond.

We perform a dynamic analysis of the Granger-causality tail risk networks of statistical fire-sales and fire-buys over the period 2003–2014. We consider a rolling-window approach with a window of three-year length¹² and one-month updates. For a given time-window t , we compute the networks with the procedure set forth in Section 2 using two-day equity returns and two-day bond yield variations, to mitigate asynchronicity effects due to the time zones. We use $(E_j \Rightarrow B_i^{\text{Sell}})_t$ and $(E_j \Rightarrow B_i^{\text{Buy}})_t$ to denote statistically significant fire-sale and fire-buy links, respectively. The subscript t is indicating that the causal networks are time-dependent since they are computed using observations prior to the end of the t th time-window.

For comparison purposes, we also compute the network with the standard Granger (1969) causality test briefly outlined in Section 2. We denote the significant links of the network as $(E_j \Rightarrow B_i)_t$, whenever the equity return of bank j Granger-causes the yield variation of bond i in mean in the t th window.

As in Billio et al. (2012), we are interested in periods in which the density of the network (also called connectedness) deviates from

¹¹ All the zero-coupon curves are elaborated, via a bootstrapping procedure representing the best-practice in the industry, by a dedicated desk of UniCredit Group.

¹² The choice of three years balances the trade-off between the power of the Granger test (as reported in the simulation study of Hong et al., 2009) and the need of localizing periods of financial distress.

¹⁰ In our analysis we adopt the Daniell kernel $k(x) = \sin(\pi x)/x$.

its expected value under the null of no-causal relationships, since this deviation may signal the presence of systemic events. As a first investigation, we define the connectedness measures

$$\begin{aligned} D_t^{\text{Sell}} &\equiv \frac{1}{N_t^E N_t^B} \sum_{j=1}^{N_t^E} \sum_{i=1}^{N_t^B} 1_{\{(E_j \Rightarrow B_i^{\text{Sell}})_t\}}, \\ D_t^{\text{Buy}} &\equiv \frac{1}{N_t^E N_t^B} \sum_{j=1}^{N_t^E} \sum_{i=1}^{N_t^B} 1_{\{(E_j \Rightarrow B_i^{\text{Buy}})_t\}}, \\ D_t &\equiv \frac{1}{N_t^E N_t^B} \sum_{j=1}^{N_t^E} \sum_{i=1}^{N_t^B} 1_{\{(E_j \Rightarrow B_i)_t\}}. \end{aligned} \quad (5)$$

where N_t^E and N_t^B represent, respectively, the total number of available equities and bond series in the t th network. D_t^{Sell} and D_t^{Buy} are the fractions of validated causal links for the significant statistical fire-sales $(E_j \Rightarrow B_i^{\text{Sell}})_t$ and fire-buys $(E_j \Rightarrow B_i^{\text{Buy}})_t$. For completeness, we also define D_t as the percentage of validated links of the Granger-causality in mean network, $(E_j \Rightarrow B_i)_t$.

Fig. 1 plots these measures of connectedness computed in each window t , along with the corresponding confidence bound. Note that, being all statistical tests performed with a confidence level of 5%, under the null of no-causality we expect to find, for the three connectedness measures, a value around 5%. Since the confidence level under the null of no-causality may be higher due to finite-sample effects or estimation errors, we compute the confidence bounds for the three measures using a bootstrap procedure described in Appendix D. The confidence bounds of D_t^{Sell} and D_t^{Buy} are slightly greater than that of D_t because of the error involved in the estimation of the VaR model and the fact that the tail-test is built from a smaller statistic.

Fig. 1 witnesses an interesting empirical evidence. If we interpret D_t^{Sell} and D_t^{Buy} as, respectively, indicators of periods of distressed selling and distressed buying, the former peaks during the Eurozone crisis while the latter during the 2007–2008 financial market crisis. This evidence suggests that the two crises are associated with different types of flight-to-quality behaviors: the first is characterized by a strong increase in sovereign bond purchases which is not accompanied by a significant (i.e. above the corresponding confidence level) rise in sovereign bond selling; while the second crisis features the contemporaneous presence of both statistical fire-buys and fire-sales of sovereign bonds.

Another interesting aspect emerging from Fig. 1 is that D_t produces a weaker signal compared to D_t^{Sell} and D_t^{Buy} , being significant only during the Eurozone crisis, and offering limited insight on the risk propagation.

4.1. An assessment of the other tail causalities

To complement the main analysis based on D_t^{Sell} and D_t^{Buy} , we investigate the structure of the Granger-causality tail risk networks for the other six possible causal relationships: $(E_j^{\text{Buy}} \Rightarrow B_i^{\text{Buy}})_t$; $(E_j^{\text{Buy}} \Rightarrow B_i^{\text{Sell}})_t$; $(B_j^{\text{Sell}} \Rightarrow E_i^{\text{Buy}})_t$; $(B_j^{\text{Sell}} \Rightarrow E_i^{\text{Sell}})_t$; $(B_j^{\text{Buy}} \Rightarrow E_i^{\text{Buy}})_t$; $(B_j^{\text{Buy}} \Rightarrow E_i^{\text{Sell}})_t$. Despite these relationships are of minor interest for us, some of them reveal interesting patterns that can be used to validate the conclusions from the main analysis.

We use a moving window scheme to build a sequence of Granger-causality tail risk networks with the procedure outlined in Section 2. To be consistent with the definition of statistical fire-buys and fire-sales introduced above, we say that equity buys imply bond buys (sales) in a statistical sense. Analogously, when reverting the causal relationship, we say that bond sales (buys) imply equity buys (sales) in a statistical sense.

From each Granger-causality tail risk network, we obtain a measure of connectedness analogous to those defined in (5). Fig. 2 shows these measures computed in each window t . A first interesting pattern is portrayed in the right panel. Bond buy implies equity sell in a statistical sense over the whole period of the analysis. Under the assumption of stability of the fundamentals, this confirms that price-mediated contagion occurred both in the 2007–2008 financial crisis and during the European debt crisis. Another interesting relationships is depicted in the middle panel. This shows that during the Eurozone crisis there was statistically significant Granger-causality in tail from bond sales to equity sales. This evidence is consistent with the fact that several banks suffered large losses following the depreciation of most of the European sovereign debts.¹³ For example, this was the case for Dexia, Société Générale and BNP Paribas as they were forced to write down the value of their Greek debt holdings. This result also reinforces our second conclusion that during the Eurozone crisis, flights-to-quality from equity to bond went with a massive liquidation of low-rated bonds.

5. Flight-to-quality

In this section we develop our econometric measure of flight-to-quality built upon the Granger causal networks previously defined. A flight-to-quality episode is commonly referred to as a conveyance of capital from risky assets to more secure ones thus accepting to receive lower expected returns. Such events are triggered by particularly distressed states of the market in which the risk aversion of investors may suddenly increase. As clearly spelled out in Anderson and Liu (Louis), [...] in times of turmoil, investors accept zero or negative nominal yields as a fee for safety.

The crucial point here is to understand which kind of quality is sought by market players in each period, thus we need to identify a proxy for the quality of a sovereign bond. For this analysis we use the historical S&P's ratings. More precisely, for each bond in the dataset, we have at our disposal the historical S&P's ratings divided into 10 different rating classes.¹⁴ We aggregate these 10 rating classes into two broad categories which we generically denote as “good” and “bad” bonds. Clearly, this broad classification will depend on how strict the definition of a “good” bond is. In order to investigate the different levels of quality requested by the market in different periods, we consider two different definitions of “good” bonds. In the first definition, that will be referred to as the *weak* definition of quality, we define “good” bonds as those with a rating between AAA and A and “bad” bonds the remaining ones. The second definition, that will be referred as the *strong* definition of quality, is more stringent since it classifies a bond as “good” only if the corresponding country has a AAA rating. For each time-window t , we define the indicator function $\mathbb{1}_{i \in \text{Good}}(t)$ as equal to one if bond i is rated in the “good” category and zero otherwise. Similarly, $\mathbb{1}_{i \in \text{Bad}}(t)$ is the indicator function that equals one if bond i is rated in the “bad” category in the time-window t and zero otherwise. The definition of bad and good in the indicator functions depends on the definition of quality that it is adopted. Hence,

¹³ This interpretation was suggested by an anonymous referee, and we thank him for pointing this out.

¹⁴ Namely: AAA, AA, A, BBB, BB, B, CCC, CC, C, SD (selectively defaulted on some obligations). The first available bond price in the time stamp may correspond to an earlier date than the first available rating for the same bond (see Table 4). If this is the case, we attach to the bond the first available rating. The impact of this attribution is negligible since we divide the bonds into two aggregated categories according to two definitions of quality.

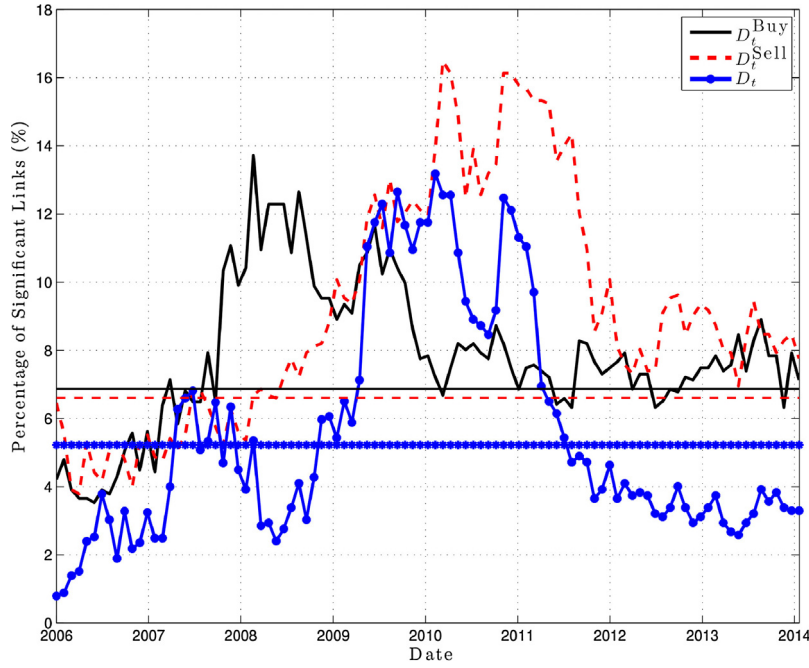


Fig. 1. Connectedness measures D_t^{Buy} , D_t^{Sell} , D_t computed as in (5) for each t th window. The dates reported in the horizontal axis correspond to the end of the time-windows used in the test. Horizontal lines are the bootstrapped 5% confidence bounds of each measure (see Appendix D).

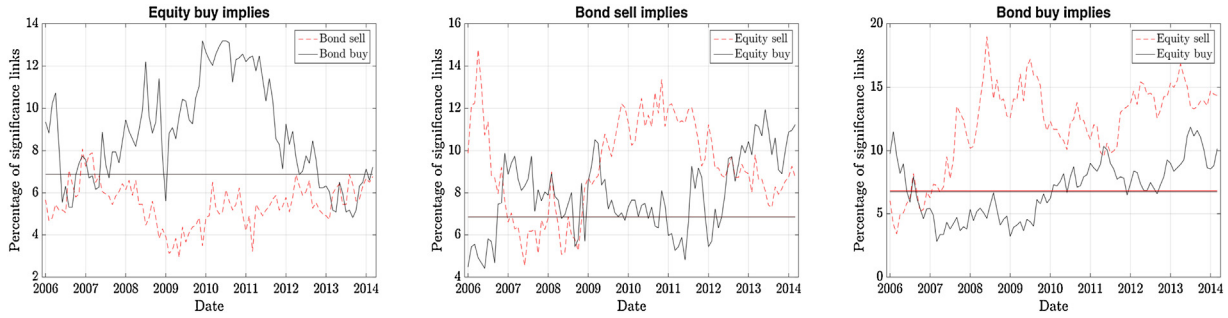


Fig. 2. Measures of connectedness from the other Granger-causality tail risk networks computed in each window t . Horizontal lines are the bootstrapped 5% confidence bounds of each measure (see Appendix D).

the weak definition produces different indicator functions than the strong one. We then consider the four quantities,

$$\begin{aligned}
 \text{Good}_t^{\text{Buy}} &\equiv \frac{\sum_{j=1}^{N_t^E} \sum_{i=1}^{N_t^B} \mathbb{1}_{\{(E_j \Rightarrow B_i^{\text{Buy}})_t\}} \mathbb{1}_{i \in \text{Good}}(t)}{N_t^E \sum_{i=1}^{N_t^B} \mathbb{1}_{i \in \text{Good}}(t)}, \\
 \text{Good}_t^{\text{Sell}} &\equiv \frac{\sum_{j=1}^{N_t^E} \sum_{i=1}^{N_t^B} \mathbb{1}_{\{(E_j \Rightarrow B_i^{\text{Sell}})_t\}} \mathbb{1}_{i \in \text{Good}}(t)}{N_t^E \sum_{i=1}^{N_t^B} \mathbb{1}_{i \in \text{Good}}(t)}, \\
 \text{Bad}_t^{\text{Buy}} &\equiv \frac{\sum_{j=1}^{N_t^E} \sum_{i=1}^{N_t^B} \mathbb{1}_{\{(E_j \Rightarrow B_i^{\text{Buy}})_t\}} \mathbb{1}_{i \in \text{Bad}}(t)}{\sum_{j=1}^{N_t^E} \sum_{i=1}^{N_t^B} \mathbb{1}_{i \in \text{Bad}}(t)}, \\
 \text{Bad}_t^{\text{Sell}} &\equiv \frac{\sum_{j=1}^{N_t^E} \sum_{i=1}^{N_t^B} \mathbb{1}_{\{(E_j \Rightarrow B_i^{\text{Sell}})_t\}} \mathbb{1}_{i \in \text{Bad}}(t)}{N_t^E \sum_{i=1}^{N_t^B} \mathbb{1}_{i \in \text{Bad}}(t)}.
 \end{aligned} \tag{6}$$

For example, $\text{Good}_t^{\text{Buy}}$ is the average number of statistical fire-buys hitting a bond of the category “Good”. These metrics can be interpreted as quality-based measures of connectedness for the statistical fire-buys and statistical fire-sales, depending on the kind of causal relationship adopted.

The left and right columns of Fig. 3 plot these quality-based measures of connectedness computed in each window t for the weak and strong definition of quality, respectively. There are two interesting aspects that need to be emphasized. First, once we identify quality with top-rated AAA bonds (top-right panel), a surge of statistical fire-buys (black continuous line) toward good bonds occurred during the 2007 financial crisis and the Eurozone crisis. This evidence is less pronounced when considering the weaker definition of quality. Second, while there is scant evidence of statistical fire-sales (red dotted line in the top-right panel) toward top rated AAA bonds, we can observe a considerable increase of statistical fire-sales during the Eurozone crisis for all the other categories (red dotted line in the bottom-right panel).

The implications of these findings are far reaching and they suggest that prominent market players did chase for quality in periods of market distress but they did it in different ways: in the first phase, during the 2007–2008 financial crisis, they chased quality by buying sovereign debt bonds particularly of top-rated AAA quality but also of AA and A quality and without simultaneously massively liquidating other lower rating bonds. As a matter of fact, only bad bonds in weak sense show a moderate amount of statistical fire-sales (bottom left panel). On the contrary, in the second phase, during the 2009–2011 Eurozone crisis, investors required

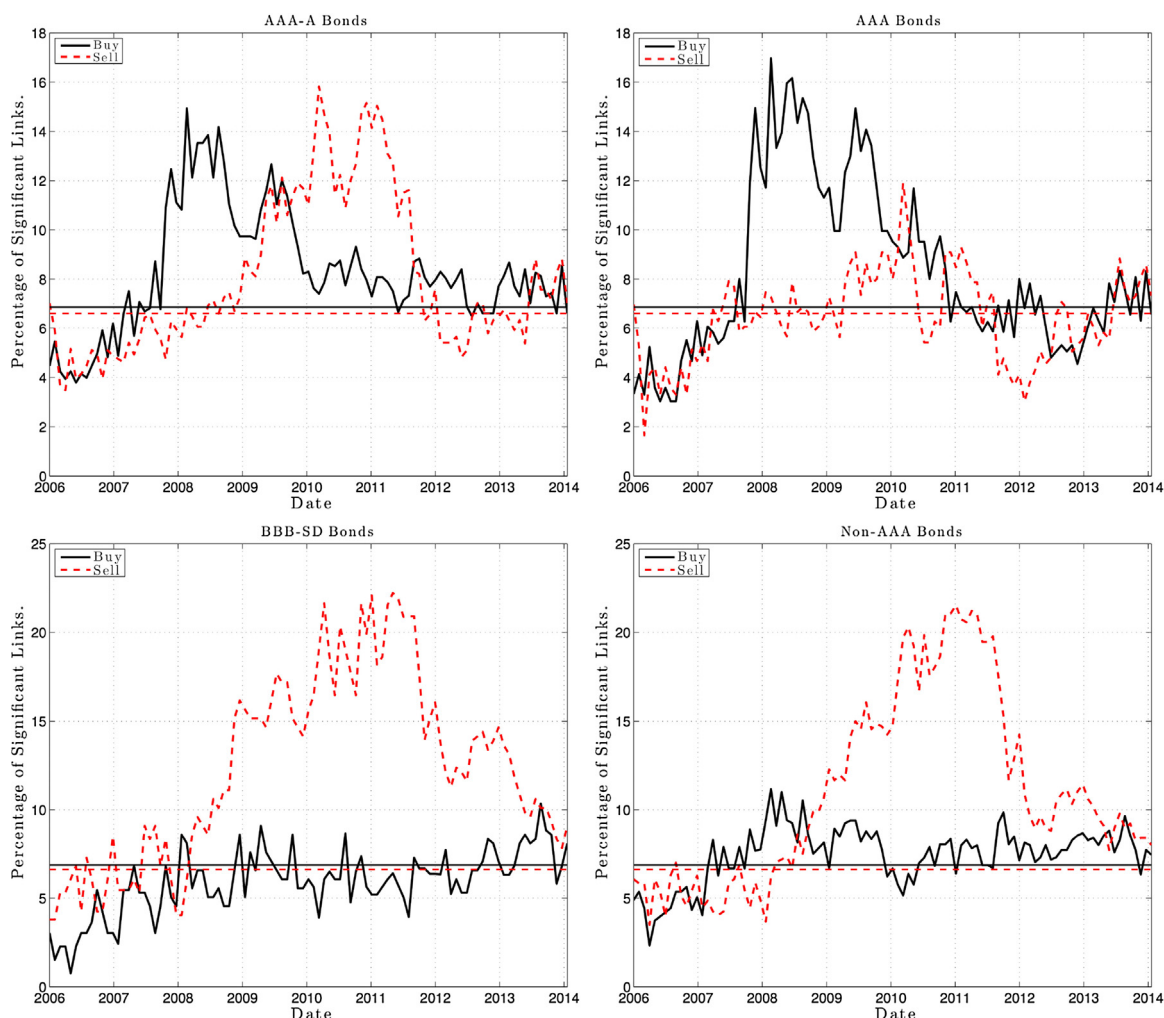


Fig. 3. Quality-based measures of connectedness for statistical fire-buys (black) and fire-sales (red-dotted), as defined in Eq. (6). The left column reports the results corresponding to the weak definition of bond quality while the right column corresponds to the strong one. Horizontal lines are the corresponding confidence bounds under the null of no causality.

only top-quality sovereign debt, i.e. the flight-to-quality occurred exclusively toward AAA-rated sovereign bonds, also at the expense of other not-AAA-rated bonds, which were simultaneously heavily liquidated.

Note that, the extraordinarily high number of hits toward the AAA, AA and A categories during the 2007–2008 financial crisis (which is manifested as the peak around mid-2008 of the black continuous curve in the top-left panel of Fig. 3), is likely to be a consequence of a flight-to-quality from toxic assets (such as subprime mortgages) to highly rated sovereign debts. However, since our dataset does not include any of the assets that were perceived as toxic during the subprime mortgage crisis, we cannot fully investigate such type of flight-to-quality.

Our analysis clearly points towards the existence of two different types of flight-to-quality: in the first one (during the 2007–2008 financial crisis) financial portfolios have been significantly rebalanced from risky equities and structured assets to sovereign bonds, while in the second one (during the 2009–2011 Eurozone crisis) sovereign bond portfolios have been rebalanced from low and medium-rated bonds to top-rated bonds. The latter could thus be termed a “flight-to-top-quality” event. In both circumstances, assets’ liquidity may also have played an important role. Under the assumption that the assets are fully liquid and that holdings of the banks cannot generate a considerable price impact, a bank will decide to rebalance its portfolio selling the assets with the high-

est risk. However, we know that the sovereign bond market is not fully liquid and, in particular, sovereign bonds with higher creditworthiness are also the more liquid (Petrella and Resti, 2017). Moreover, our analysis is based on 33 G-SIBs institutions, therefore we cannot exclude possible price impacts when selling large amounts of marketable assets. Under these conditions, the decision of which assets to liquidate first is more complicated, either in the case of banks pursuing a leverage target (Greenwood et al., 2015; Cont and Schaanning, 2017) or complying with a risk-based capital ratio constraint (Braouezec and Wagalath, 2016), and optimal liquidation rules will depend on the risk of generating liquidity spirals following consecutive assets depreciations. These considerations may account for the fact that small amounts of good quality bonds were sold during the European debt crisis while statistical fire-sales of bad bonds were mounting. The advantage of our method is that it does not require explicitly the measurement of liquidity to assess price-mediated contagion and the associated systemic risk, even if we are implicitly using a notion of liquidity by separating the bonds into rating classes.

The hypothesis of occurrence of different flight-to-quality episodes suggested by the plots of Fig. 3 can be statistically validated comparing the number of hits per category with that expected under the null in which links from equities to bonds are randomly assigned. The computation of these expected values under the null is straightforward: if bonds were randomly hit by

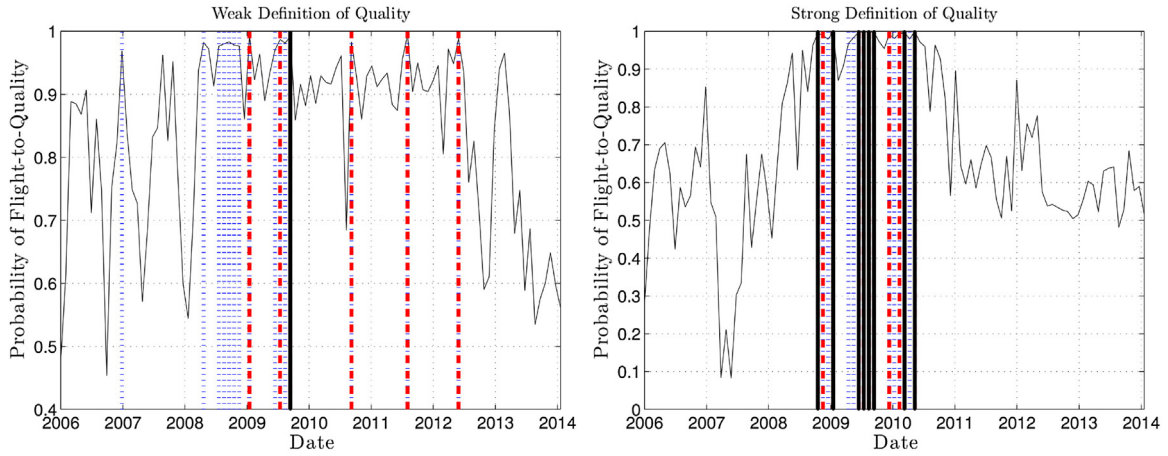


Fig. 4. The figure shows the proposed flight-to-quality measure. Vertical lines are in correspondence of time-windows in which both $p_{Good,t}^{Buy}$ and $p_{Bad,t}^{Sell}$ are above a threshold p , which is fixed to 99% for the continuous black vertical lines, to 97.5% for the thick red dotted lines and to 95% for thin dotted blue lines. The thin black curve represents the quantity $(p_{Good,t}^{Buy} + p_{Bad,t}^{Sell}) / 2$, that is the arithmetic mean of the two probabilities. (For interpretation of the references to color in this legend, the reader is referred to the web version of the article.)

equities without any preference toward a specific category, then the probability of observing less than $N_{Good,t}^{Buy}$ hits is given by the cumulative binomial distribution

$$P_{Good,t}^{Buy} = \sum_{k=0}^{N_{Good,t}^{Buy}} \binom{N_{Good,t}^{Buy}}{k} p_{Good,t}^k (1 - p_{Good,t})^{N_{Good,t}^{Buy} - k}, \quad (7)$$

where

$$p_{Good,t} = \frac{\sum_{i=1}^{N_t^B} \mathbb{1}_{i \in \text{Good}}(t)}{N_t^B}$$

is the probability of having a good rated bonds at time t and where $N_t^{Buy} = \sum_{j=1}^{N_t^E} \sum_{i=1}^{N_t^B} (E_j \Rightarrow B_i^{Buy})_t$, is the total number of significant $(E_j \Rightarrow B_i^{Buy})_t$ links. The computation of $p_{Bad,t}^{Sell}$ and the other probabilities follows the same rule. When the probability in (7) is larger than a threshold p (e.g. $p = 99\%$), it means that there is a statistically significant number of statistical fire-buys toward good rated bonds. A similar reasoning applies for the bad rated ones and statistical fire-sales. We identify a *statistical flight-to-quality* when both $p_{Good,t}^{Buy}$ and $p_{Bad,t}^{Sell}$ exceed a large probability p simultaneously. Results of the flight-to-quality test are reported in Fig. 4 distinguishing, as before, between the two definitions of good and bad bonds. The left panel corresponds to the weak definition where good bonds are those in the class from AAA to A, while the right panel corresponds to the strong definition of quality where a bond is classified as good only if the country has a AAA rating. The vertical thick lines are in correspondence of the periods in which our test identifies a statistical flight-to-quality. They are distinguished into three cases, continuous black vertical lines correspond to $p = 99\%$, thick red dotted lines to $p = 97.5\%$ and thin dotted blue lines to $p = 95\%$.

The scenario depicted by the results of Fig. 4 confirms the intuition that we got from the preliminary analysis inspired by the plots in Fig. 3. Quality is required as a consequence of the turmoil and distrust spread by the Eurozone crisis, and the phenomenon is well-identified if quality is defined by top-quality AAA-rated bonds. In fact, with the weak definition of quality, we find only one highly significant period of statistical flight-to-quality after mid-2009 and many other less significant scattered all around the time stamp. On the contrary, the strong definition gives a concentrated sequence of highly significant events around the Eurozone crisis and even before the beginning of 2009.

Each panel of Fig. 4 reports the arithmetic mean between $p_{Good,t}^{Buy}$ and $p_{Bad,t}^{Sell}$. Using a strong definition of quality, one can note that this quantity shows an upward trend since the mid-2007, much before the onset of the Eurozone crisis, and peaks some months before 2009, signaling the changing market conditions. We consider this an indicator of statistical flight-to-quality that can extend the tool kit available to a policymaker interested in the stability of the financial system. It adds valuable information, beyond those provided by systemic-risk measures based on asset prices, indices of market volatility, the TED spread, and other traditional measures of financial distress. In particular, our indicator of statistical flight-to-quality offers a unique perspective on the bank-bond system, focusing on the causal relationship between extreme events. This allows surveillance authorities to take targeted actions directed to suppress moments of instability in this system.

6. Out-of-sample forecasts of bond quality

We perform an out-of-sample analysis to assess whether suitable centrality measures of the Granger-causality networks can be used to predict sovereign bond quality.

6.1. Dynamic proxies of quality

We consider four proxies of sovereign bond quality that are defined “dynamically” in the sense of a continuous, time-dependent, real variable. Agency rating are not well-suited for our purpose because they are almost constant during time and, when they change, they signal a huge downgrade or, more rarely, a huge upgrade of the sovereign debt quality. For a given country, the first proxy is based on the correlation between the series of sovereign bond yields and the corresponding credit default swap. A simple absence of arbitrage argument links the spread S of CDS with the par-yield γ of a bond of the same entity. As pointed out by Hull et al. (2004), the difference between a CDS spread and the corresponding par-yield should equal the risk-free rate r , in formula

$$S = \gamma - r. \quad (8)$$

The difference between a CDS spread and the excess par-yield over the risk-free rate, $b = S - (\gamma - r)$, is usually referred as the basis. Hence, the no-arbitrage condition requires the basis to be zero. On a large sample of companies and sovereign data, Hull et al. (2004) find that the no-arbitrage relationship between CDS and par-yield

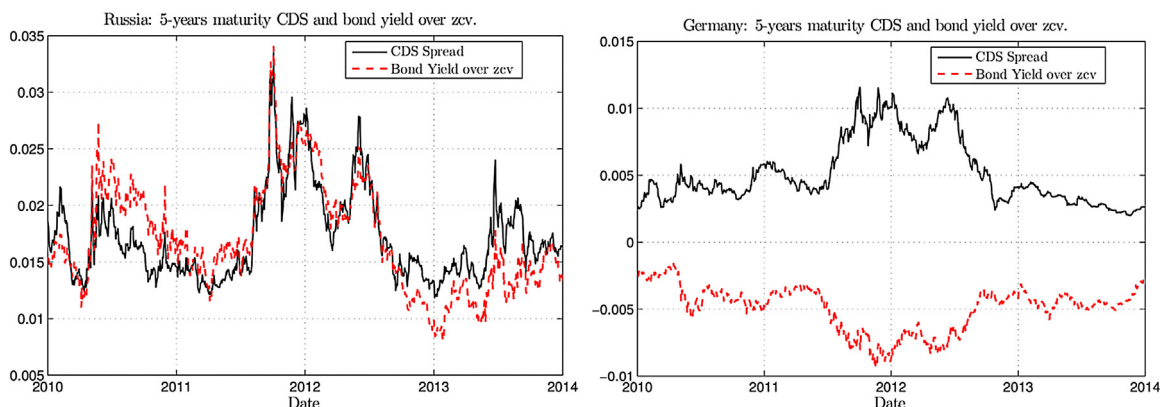


Fig. 5. Left and right panels report, respectively, the five-years maturity spread (continuous black line) and bond yield over the zero-coupon curve (dotted red line) for Russia and Germany in the period that starts in January, 1, 2007 and ends at February, 14, 2014. (For interpretation of the references to color in this legend, the reader is referred to the web version of the article.)

holds fairly well, with a risk-free rate slightly smaller than the swap rate and above the Treasury rate. In our dataset¹⁵ we observe that, especially in periods of financial distress, such arbitrage relationship could be violated, particularly for those countries whose credit quality is commonly perceived as remarkably good.

Fig. 5 visualizes this phenomenon. The left and right panels report the five-years maturity CDS spread (continuous black line) and the corresponding five-years maturity sovereign bond yield (dotted red line) for Russia and Germany, respectively. The bond yield reported is the nominal par-yield after the subtraction of the zero-coupon curve, that according to the no-arbitrage condition (8) should be equal to the CDS spread. The period depicted includes the Eurozone crisis. The plots in Fig. 5 put in evidence that, while Russia has a CDS-bond correlation of almost 100%, in agreement with the no-arbitrage constraint, the case of Germany is totally different, showing even a negative CDS-bond correlation. Intuitively, CDS spreads increase during a period of crisis since investors require higher premiums, however the behavior of bond yield can be very different according to the perceived credit quality of the country. The case of Germany is the most striking: large capital flows are directed toward the German sovereign debt pushing downward the level of the corresponding yield, while the CDS spread continues its rise as a consequence of the generalized increase in global credit risk. This empirical evidence has been somehow foreseen by the past literature. In fact, price gaps among securities with identical cash flow have been theoretically justified by the general equilibrium model by Gârleanu and Pedersen (2011), where the surge of the CDS-bond basis is due to negative shocks to the economy that force agents to hit their margin constraints. Moreover, the formation of CDS-bond bases has been recently addressed as a consequence of flight-to-quality episodes by Fontana and Scheicher (2016).

In our analysis we do not investigate the determinants of CDS-bond bases, limiting ourselves to the ranking of bond quality obtained by using the CDS-bond correlation. In the light of the empirical evidences of Fig. 5 and the most recent interpretation of the CDS-bond joint dynamics, we introduce our first dynamical proxy for quality of the bond i as

$$C_i = 1 - \text{Corr} [\Delta\gamma_{i,t}, \Delta S_{i,t}], \quad C_i \in [0, 2], \quad (9)$$

where the capital letter C is introduced to remind that the quality proxy is based on the CDS-bond correlation¹⁶ coefficient and where $\Delta\gamma_{i,t}$ and $\Delta S_{i,t}$ indicates, respectively, the series of one-lag difference for $\gamma_{i,t}$ and $S_{i,t}$.

The first column of Table 1 reports the country ranking according to the quality measure C_i , computed using all observations after the beginning of 2007. As anticipated, we observe a clear alignment between the country and what it is intuitively expected: countries with weak fiscal discipline (e.g. Spain, Italy and Portugal) stay in the bottommost part of the table with very low values of C_i , while the largest values are reached for countries such as Germany or Austria, whose claims on sovereign debts are undoubtedly perceived as more reliable. The case of Greece is not particularly significant since the corresponding CDS series show a very peculiar behavior, with a diverging dynamics during the Eurozone crisis.

In order to have a multifaceted description of the bond quality, we introduce three further measures that are obtained exclusively using the bond yields time series. The simplest univariate measure related to bond quality is the bond yield “realized volatility”, defined as

$$RV_i = \sum_{t \geq 2007} (\Delta\gamma_{i,t})^2,$$

where $\gamma_{i,t}$ indicates the daily series of the nominal bond yield for country i . The larger the value of RV_i the greater the uncertainty about its value, hence we expect RV_i to be inversely related to bond quality. This intuition is confirmed by the second column of Table 1, where countries are ranked according to increasing values of RV_i , with Japan being the less volatile and Greece at the end of the ranking.

The remaining two measures are based on yield spreads defined in the standard way, i.e. the difference between a given sovereign bond yield and the corresponding German bond yield at the same maturity (which is, in our applications, five years). The introduction of yield spreads in our analysis is justified by the vast literature on the role of spreads in many aspects of the global economy. For example, the prominent role of spreads in the European Monetary Union as a source of risk is analyzed, much before the Eurozone crises, by Geyer et al. (2004) with the adoption of a two-factor model. Moreover, Manganeli and Wolswijk (2009) investigate the relationship between macro-economic policies and yield spreads.

¹⁶ Note that in Eq. (9) we are not specifying which time period is used for the two series $\Delta\gamma_{i,t}$ and $\Delta S_{i,t}$, nevertheless this will become clear according to the specific case.

¹⁵ Our dataset has almost zero time overlap with that of Hull et al. (2004).

Table 1
Ranking of country according to quality proxies.

C_i		RV_i		\bar{S}_i		SM_i	
1.275	Germany	0.933	Japan	-2.453	Switzerland	-1.054	Singapore
1.149	Australia	1.885	Switzerland	-2.242	Singapore	-0.855	Switzerland
1.115	Denmark	3.119	Singapore	-1.828	Hong Kong	0.000	Germany
1.113	Sweden	3.832	New Zealand	-1.531	Japan	0.008	Japan
1.111	Romania	4.264	Sweden	-1.241	United States	0.563	Hong Kong
1.075	Czech Rep.	4.390	Finland	-1.199	Finland	0.861	Netherlands
1.069	United Kingdom	4.475	Hong Kong	-1.085	France	1.201	Denmark
1.062	Norway	4.643	Netherlands	-0.785	Sweden	1.341	United Kingdom
1.042	United States	4.797	Denmark	-0.130	Canada	1.454	Sweden
1.029	Japan	4.849	Canada	-0.100	Malaysia	1.733	Norway
1.025	Singapore	4.886	Norway	0.000	Germany	1.910	Canada
1.004	Bulgaria	4.911	France	0.016	Slovakia	2.080	Austria
0.993	New Zealand	4.964	Poland	0.178	Denmark	2.095	United States
0.976	Finland	5.079	Czech Rep.	0.208	Italy	2.115	Finland
0.967	Hong Kong	5.105	Germany	0.238	Netherlands	2.129	France
0.959	Canada	5.170	United Kingdom	0.404	Austria	2.374	Slovakia
0.944	Switzerland	5.171	Austria	0.509	United Kingdom	2.411	Czech Rep.
0.937	Malaysia	6.325	Croatia	0.588	Poland	2.622	Malaysia
0.936	Turkey	6.442	Belgium	0.700	Bulgaria	3.097	New Zealand
0.885	Netherlands	7.187	Slovakia	0.700	Belgium	3.121	Poland
0.880	Slovakia	8.343	Australia	0.767	Czech Rep.	3.703	Italy
0.846	Hungary	8.436	United States	0.874	Norway	3.792	Australia
0.777	Poland	9.072	Malaysia	1.012	New Zealand	4.103	Belgium
0.746	Greece	10.803	Slovenia	1.680	Spain	5.044	Bulgaria
0.705	Austria	14.926	Italy	1.854	Slovenia	5.640	Slovenia
0.645	Croatia	15.161	Spain	2.300	Portugal	6.561	Croatia
0.642	Cyprus	21.824	Hungary	2.383	Russia	6.705	Russia
0.591	France	23.646	Russia	2.415	Australia	6.981	Spain
0.553	Slovenia	27.438	Ireland	2.484	Ireland	8.790	Hungary
0.544	Russia	68.692	Portugal	2.849	Hungary	9.939	Romania
0.369	Belgium	70.947	Venezuela	2.934	Croatia	14.043	Ireland
0.339	Ireland	71.989	Romania	3.940	Cyprus	15.454	Cyprus
0.337	Venezuela	85.221	Turkey	3.994	Romania	16.812	Portugal
0.327	Portugal	88.153	Bulgaria	7.974	Turkey	18.306	Venezuela
0.249	Italy	108.341	Cyprus	9.040	Venezuela	19.843	Turkey
0.220	Spain	846.110	Greece	11.406	Greece	55.484	Greece

Note: Each of the four panels contains the ranking of all countries according to the corresponding variable reported in the column label. Each variable is computed using all data available after 2007. More precisely, C_i is defined as $1 - \rho_i$ where ρ_i is the sample correlation between the sovereign bond yield and the CDS spread (and it is plotted in decreasing order). RV_i is the realized volatility of bond yield variations. \bar{S}_i and SM_i are the mean and maximum value of the spread between the bond of the i th country and the German bond, respectively.

Their empirical findings confirm that changes in interest rates affect the risk-aversion of investors producing a significant impact on yield spreads. Global spreads and fiscal fundamentals of the euro area are used to proxy expected exchange rate devaluation in an econometric model for euro area spread by Favero (2013). De Santis (2014) identifies a flight-to-liquidity premium as the only factor that explains the sovereign spreads for countries with low credit risk such as Netherlands and Finland.

The yield spread is formally defined as $S_{i,t} = \gamma_{i,t} - \gamma_{GER,t}$, where $\gamma_{GER,t}$ is the bond yield for Germany. The spread-based measures that we adopt are the average and the maximum spread after January, 1, 2007, defined as

$$\bar{S}_i = \frac{1}{N_i} \sum_{t \geq 2007} S_{i,t}, \quad \text{and} \quad SM_i = \max_{t \geq 2007} S_{i,t},$$

with N_i the number of observations for the i th series. Note that, as for RV_i , the spread-based measures are expected to be inversely related to quality. This is confirmed by the third and fourth columns of Table 1 where, typically, we observe countries like Greece or Portugal with the highest values of the spread-based measures and Switzerland, Singapore and Netherlands among the lowest ones.¹⁷

6.2. Out-of-sample cross-sectional regressions

We perform out-of-sample regressions that follow, in spirit, the approach proposed in Billio et al. (2012). For a given time-window t and a given sovereign bond i , we define the three centrality measures,

$$H_{i,t}^{Sell} \equiv \frac{1}{N_t^E} \sum_{j=1}^{N_t^E} \mathbb{1} \{ (E_j \Rightarrow B_i^{Sell})_t \}, \quad H_{i,t}^{Buy} \equiv \frac{1}{N_t^E} \sum_{j=1}^{N_t^E} \mathbb{1} \{ (E_j \Rightarrow B_i^{Buy})_t \},$$

$$H_{i,t} \equiv \frac{1}{N_t^E} \sum_{j=1}^{N_t^E} \mathbb{1} \{ (E_j \Rightarrow B_i)_t \}, \quad (10)$$

which, in network terms, are the degrees of the i th bond node. The economic interpretation of $H_{i,t}^{Sell}$ and $H_{i,t}^{Buy}$ is straightforward. The index $H_{i,t}^{Sell}$ (resp. $H_{i,t}^{Buy}$) is the percentage of significant causal links ($E_j \Rightarrow B_i^{Sell}$) (resp. $E_j \Rightarrow B_i^{Buy}$) coming from the equity side of the network that hit the i th bond in the time-window t . Large values of $H_{i,t}^{Sell}$ (resp. $H_{i,t}^{Buy}$) are expected when the i th bond has experienced several large losses (resp. gains) in the t th window, after a considerable equity drop of a large sub-sample of the 33 systemically relevant banks. The economic interpretation of $H_{i,t}$ is less direct, since it is expression of causality relationships in mean. Nevertheless, we include it in the analysis for comparison purposes.

¹⁷ Germany has trivially a zero value for all these spread-based measures.

Nested models comparison with dependent variable $C_{i,t}$.

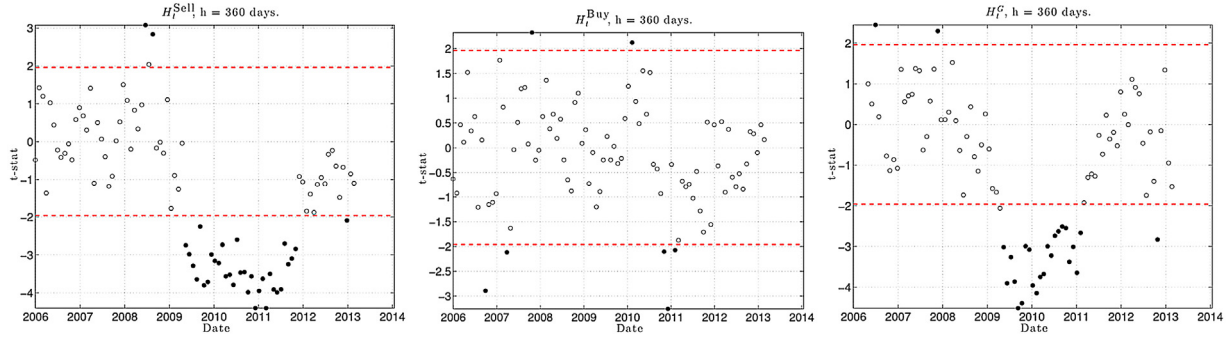


Fig. 6. Nested models comparison with dependent variable $C_{i,t}$. This figure depicts, for each time-window $t = 1, \dots, 99$ ending at day e_t (reported in the horizontal axis), the t -statistic of β_t in (13) where the dependent variable $Y_{i,t}$ is the ranking of the variable $C_{i,t}^H$ defined in (11) and computed in the forecasting horizon $(e_t, e_t + h]$, with $h = 360$. Each column corresponds to a different regressor $X_{i,t}$ in (13). More precisely, $X_{i,t} = H_{i,t}^{\text{Sell}}$ for the first, $X_{i,t} = H_{i,t}^{\text{Buy}}$ for the second and $X_{i,t} = H_{i,t}^C$ for the third. A black point is reported whenever the regression (13) is significantly better (according to a standard F -test with 95% confidence) than the simple auto-regressive model (12). Horizontal red dotted lines are in correspondence of 95% confidence level of the standard Normal distribution. (For interpretation of the references to color in this legend, the reader is referred to the web version of the article.)

We adapt the definitions of the four quality proxies introduced above in order to perform genuine out-of-sample forecasts. For this purpose, we dynamically compute the quality proxies over a moving window $(t, t+h]$ with h the number of days ahead over which the forecast is performed. Then, the four quality proxies are dynamically restated as

$$\begin{aligned}
 C_{i,t+h} &= 1 - \text{Corr}[\Delta\gamma_i, \Delta S_i]_{t:t+h}, \\
 RV_{i,t+h} &= \sum_{\tau=t}^{t+h} (\Delta\gamma_{i,\tau})^2, \\
 \bar{S}_{i,t+h} &= \frac{1}{h} \sum_{\tau=t}^{t+h} S_{i,\tau}, \\
 SM_{i,t+h} &= \max_{\tau \in (t,t+h]} S_{i,\tau}.
 \end{aligned} \tag{11}$$

Similarly to what it is done in Billio et al. (2012), in order to mitigate the effect of outliers (see, for example, the case of Greece in Table 1), we switch to the rankings of those measures introducing calligraphic notation for all the variables involved. For example $H_{i,t}^{\text{Sell}}$ indicates the ranking of $H_{i,t}^{\text{Sell}}$ in the t th time-window, $\bar{S}_{i,t}$ will indicate the ranking of $\bar{S}_{i,t}$, and so on.

The out-of-sample regressions that we run are designed to test if, especially in periods of distress, the cross-sectional rankings of the bond quality proxies can be predicted by past network centrality measures. Since each of the dynamical proxies of quality is expected to be persistent (or strongly persistent in the case of realized volatility) it is important, to avoid spurious results, to include the lagged value of the dependent variable in the forecasting regression. It is also important to stress that, at any point in time, the regressors (i.e. the centrality measures (10) and the lagged dependent variable) and the dependent variables (one of the quality proxies (11)) are computed over time windows that do not overlap. More precisely, the regressors are computed on the past time horizon $(t-h, t]$ for the lagged dependent variable, and using the three years preceding t for the network centrality measures. The regressors are indicated with the subscript t , while the chosen dependent variable (i.e. one among the four quality proxies) is calculated over the forecasting period $(t, t+h]$ and denoted with the subscript $t+h$.

In our analysis we adopt a twofold strategy. First, for every t , we run the two nested cross-sectional regressions

$$Y_{i,t+h} = K^{(1)} + \alpha_t Y_{i,t} + \varepsilon_i^{(1)} \tag{12}$$

and

$$Y_{i,t+h} = K^{(2)} + \alpha_t Y_{i,t} + \beta_t X_{i,t} + \varepsilon_i^{(2)}, \tag{13}$$

where $Y_{i,t}$ is the ranking of one among $C_{i,t}$, $RV_{i,t}$, $\bar{S}_{i,t}$ and $SM_{i,t}$ defined in (11), while the independent variable $X_{i,t}$ is the ranking of one among the centrality measures defined in (10). In this setting, we are testing whether the addition of the network-based systemically relevant variable $X_{i,t}$ in (13) is improving the simple auto-regression (12).

The second approach consists in comparing, for a given proxy of the i th bond quality $Y_{i,t+h}$ computed in the forecasting horizon $(t, t+h]$, the forecasting ability of past values of the dependent variable itself against that of the systemic risk variables. For a given t we then compare the cross-sectional regression (12) with a new regression where the lagged dependent variable is substituted by one of the systemic relevant variables, that is

$$Y_{i,t+h} = K^{(2')} + \beta'_t X_{i,t} + \varepsilon_i^{(2')}. \tag{14}$$

For this regression we compute the t -statistics of β'_t and the p -value of the Vuong (1989) likelihood ratio test.¹⁸ Since, as mentioned before, the dependent variables $Y_{i,t}$ are typically persistent, we expect that only in some peculiar periods the systemic relevant variates over-perform the past values of $Y_{i,t}$ in forecasting future values of $Y_{i,t+h}$.

6.3. Results

Regression results for $h = 360$ are depicted in Figs. 6–10.¹⁹ In particular, Figs. 6–9 report the t -statistics of the regression coefficient β_t in (13) for the regressions with dependent variable, $C_{i,t}$, $RV_{i,t}$, $SM_{i,t}$, and $\bar{S}_{i,t}$ respectively. Black points are in correspondence of the regressions in which, according to a standard F -test with 95% confidence, the addition of $X_{i,t}$ significantly improves the simple auto-regressive model (12). Fig. 10 reports the t -statistic of β'_t in (14) obtained when the dependent variable is the quality proxy based on the bond-CDS correlation. Black points mark the regressions outperforming the baseline specification in (12) according to the Vuong (1989) likelihood ratio test.

¹⁸ The test is two-sided and it is designed to be around 100% when model (12) outperforms model (14) and around 0% the other way round.

¹⁹ Results with different h are similar and available upon request.

Nested models comparison with dependent variable $\mathcal{RV}_{i,t}$.

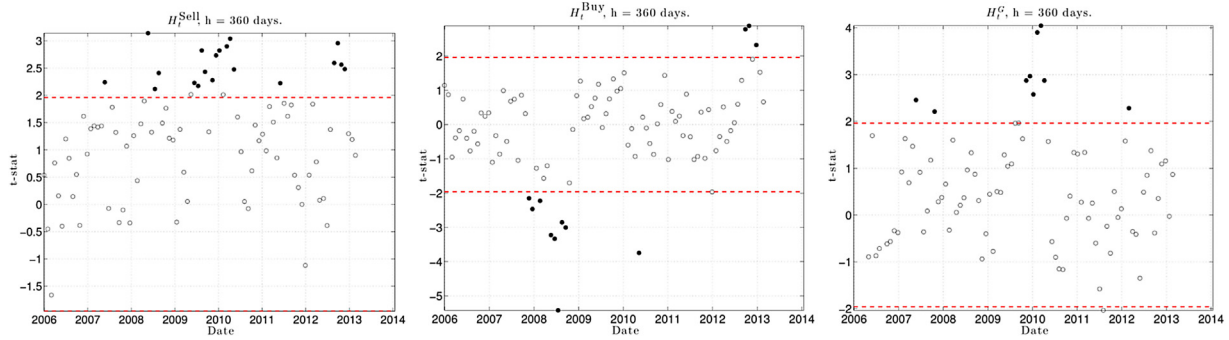


Fig. 7. Nested models comparison with dependent variable $\mathcal{RV}_{i,t}$. This figure depicts, for each time-window $t = 1, \dots, 99$ ending at day e_t (reported in the horizontal axis), the t -statistic of β_t in (13) where the dependent variable $Y_{i,t}$ is the ranking of the variable $\mathcal{RV}_{i,t}^H$ defined in (11) and computed in the forecasting horizon $(e_t, e_t + h]$, with $h = 360$. Each column corresponds to a different regressor $X_{i,t}$ in (13). More precisely, $X_{i,t} = H_{i,t}^{\text{Sell}}$ for the first, $X_{i,t} = H_{i,t}^{\text{Buy}}$ for the second and $X_{i,t} = H_{i,t}$ for the third. A black point is reported whenever the regression (13) is significantly better (according to a standard F -test with 95% confidence) than the simple auto-regressive model (12). Horizontal red dotted lines are in correspondence of 95% confidence level of the standard Normal distribution. (For interpretation of the references to color in this legend, the reader is referred to the web version of the article.)

Nested models comparison with dependent variable $\mathcal{SM}_{i,t}$.

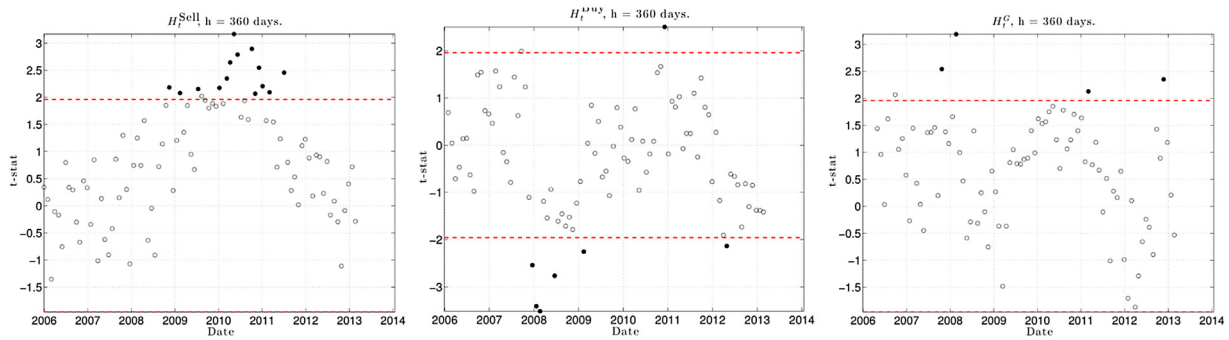


Fig. 8. Nested models comparison with dependent variable $\mathcal{SM}_{i,t}$. This figure depicts, for each time-window $t = 1, \dots, 99$ ending at day e_t (reported in the horizontal axis), the t -statistic of β_t in (13) where the dependent variable $Y_{i,t}$ is the ranking of the variable $\mathcal{SM}_{i,t}^H$ defined in (11) and computed in the forecasting horizon $(e_t, e_t + h]$, with $h = 360$. Each column corresponds to a different regressor $X_{i,t}$ in (13). More precisely, $X_{i,t} = H_{i,t}^{\text{Sell}}$ for the first, $X_{i,t} = H_{i,t}^{\text{Buy}}$ for the second and $X_{i,t} = H_{i,t}$ for the third. A black point is reported whenever the regression (13) is significantly better (according to a standard F -test with 95% confidence) than the simple auto-regressive model (12). Horizontal red dotted lines are in correspondence of 95% confidence level of the standard Normal distribution. (For interpretation of the references to color in this legend, the reader is referred to the web version of the article.)

Nested models comparison with dependent variable $\bar{\mathcal{S}}_{i,t}$.

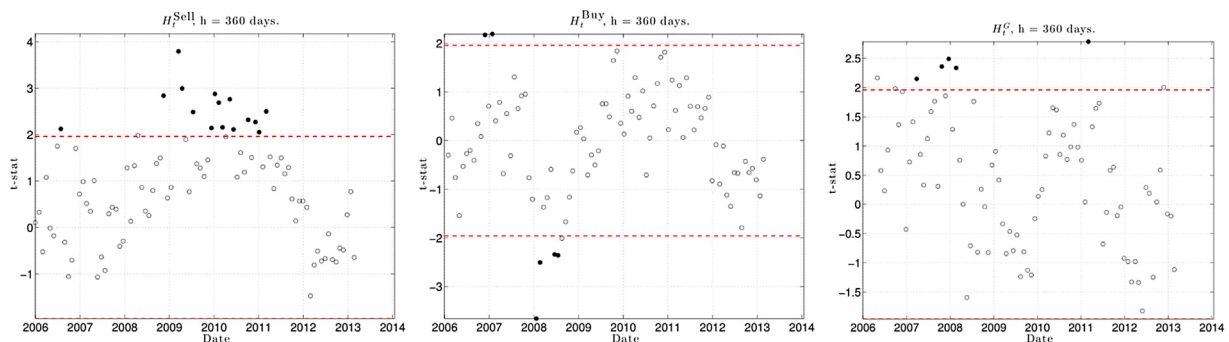


Fig. 9. Nested models comparison with dependent variable $\bar{\mathcal{S}}_{i,t}$. This figure depicts, for each time-window $t = 1, \dots, 99$ ending at day e_t (reported in the horizontal axis), the t -statistic of β_t in (13) where the dependent variable $Y_{i,t}$ is the ranking of the variable $\bar{\mathcal{S}}_{i,t}$ defined in (11) and computed in the forecasting horizon $(e_t, e_t + h]$, with $h = 360$. Each column corresponds to a different regressor $X_{i,t}$ in (13). More precisely, $X_{i,t} = H_{i,t}^{\text{Sell}}$ for the first, $X_{i,t} = H_{i,t}^{\text{Buy}}$ for the second and $X_{i,t} = H_{i,t}$ for the third. A black point is reported whenever the regression (13) is significantly better (according to a standard F -test with 95% confidence) than the simple auto-regressive model (12). Horizontal red dotted lines are in correspondence of 95% confidence level of the standard Normal distribution. (For interpretation of the references to color in this legend, the reader is referred to the web version of the article.)

Non-nested models comparison with dependent variable $C_{i,t}$.

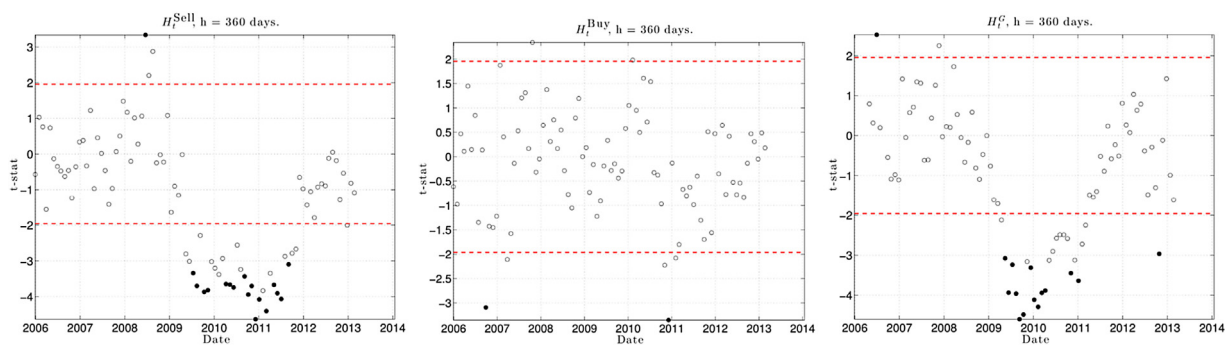


Fig. 10. Non-nested models comparison with dependent variable $C_{i,t}$. This figure depicts, for each time-window $t = 1, \dots, 99$ ending at day e_t (reported in the horizontal axis), the t -statistic of β_i^t in (14) where the dependent variable $Y_{i,t}$ is the ranking of the variable $C_{i,t}^H$ defined in (11) and computed in the forecasting horizon $(e_t, e_t + h]$, with $h = 360$. Each column corresponds to a different regressor $X_{i,t}$ in (14). More precisely, $X_{i,t} = H_{i,t}^{\text{Sell}}$ for the first, $X_{i,t} = H_{i,t}^{\text{Buy}}$ for the second and $X_{i,t} = H_{i,t}^C$ for the third. A black point is reported whenever the regression (14) is significantly better (according to the log-likelihood ratio test of Vuong (1989) with 95% confidence) than the simple auto-regressive model (12). Horizontal red dotted lines are in correspondence of 95% confidence level of the standard Normal distribution. (For interpretation of the references to color in this legend, the reader is referred to the web version of the article.)

The results can be summarized in three main empirical findings. First, the black points in Fig. 6 document a significant negative impact of $H_{i,t}^{\text{Sell}}$ on future values of the CDS-bond correlation rankings. This means that the bond quality ranked according to C_i is, in period of financial distress, significantly influenced by the intensity of statistical fire-sales experienced by the bond in the past years. The negative sign is in agreement with the idea that high values of C_i correspond to a better quality for the bond (see Table 1). On the contrary, statistical fire-buys have no influence on future values of C_i . Moreover, as for the results in Fig. 1, the regressions for $H_{i,t}$ are roughly in agreement with those of the statistical fire-sale indicator. The non-nested analysis reported in Fig. 10 corroborates the results of Fig. 6, with the intriguing implication that, during periods of financial turmoil, systemic variables are more informative than past values of quality measures in predicting the future quality of the bonds. Second, the realized volatility of bond yields is positively and significantly impacted by $H_{i,t}^{\text{Sell}}$, particularly during the Eurozone crisis, and by $H_{i,t}^C$. The statistical fire-buy indicator $H_{i,t}^{\text{Buy}}$ shows a noisier behavior, even if it tends to show a negative sign when significant (as intuitively expected) over most part of the sample (turning positive only in the final periods). Third, the maximum spread is largely influenced by $H_{i,t}^{\text{Sell}}$ for the entire period of the Eurozone crisis and even later.

Summing up, the connectedness measures obtained from the Granger-causality tail risk network of statistical fire-sales have a strong impact on the future values of the bond quality, and they add statistically insightful information beyond that provided by classical risk indicators such as the realized volatility of the bond's yield, the CDS-bond correlation, and the yield spread.

7. Conclusions

We introduced an econometric method designed to detect and analyze periods of financial distress based on events of extraordinary nature. We use the test of Granger-causality in tail of Hong et al. (2009) to build Granger-causality tail risk networks between equity log-returns of 33 systemically relevant banks and government bond yield variations for 36 countries around the world. We derive measures of centrality for these networks that we economically interpret, under the assumption of stable fundamentals, as indicators of statistical fire-buys and statistical fire-sales. Exploit-

ing the information of S&P country ratings, our empirical analysis evidences that, during the turbulent period of the Eurozone crisis, the sovereign bond market has been impacted by investors chasing for quality. More specifically, top-quality bonds have incurred in large negative variations of their yields (price increases), and this happened with a simultaneous dramatic loss of value for the large part of non-AAA-rated bonds. Besides, statistical fire-buys toward AAA-rated bonds largely occurred during the subprime mortgages crisis. Although, we do not have specific information on assets which were classified as toxic during the 2007 financial crisis, it is very likely that the surge of the statistical fire-buy index for AAA-rated bonds is due to flight-to-quality episodes from the stock market to the government bond market. The interpretation of our results is multifaceted and connected to those of Baur and Lucey (2009). While the results of Baur and Lucey (2009) document the appearance of flight-to-quality from stocks (indexes) and bonds (indexes) on several countries (and also on contagion among countries) during major financial crises, we put the focus on flight-to-quality within the sovereign bond markets and from stocks of major financial banks to highly-rated sovereign bonds. Most importantly, as mentioned in the Introduction, in our econometric framework it is not necessary to know the temporal positioning of the financial crises *ab initio*, since crises are automatically identified by the simultaneous occurrence of large equity drops for a considerable fraction of the systemically relevant banks.

Finally, adopting different dynamic proxies of bond quality allows us to test whether the centrality measures can predict the ranking of creditworthiness of the sovereign bonds. The indicator of statistical fire-sale has significant explanatory power in forecasting future values of the correlation between CDS spreads and the bond yield of a country, of the yield realized volatility and of the maximum spread with respect to the German bond. The behavior of the centrality measure based on the original Granger (1969) causality, although with a reduced forecasting power, is in line with the indicator of statistical fire-sale. In summary, we show that it is possible, during periods of crises, to improve the forecast of the future (perceived) quality ranking of sovereign bonds. We believe that this is an appealing feature of our measures, since they could provide insightful information to surveillance authorities in the very moment their intervention is needed for the financial stability of the sovereign debt market.

Table 2
Parameter estimates of the model (16) for daily time series of sovereign bond yield variations.

	Country Bond											
	AUSTRALIA	BULGARIA	CANADA	SWITZERLAND	CZECH REPUBLIC	DENMARK	AUSTRALIA	BELGIUM	CROATIA	CYPRUS	FINLAND	FRA
β_1	0.0031 (0.08)	0.0243 (0.00)	0.0002 (0.38)	-0.0007 (0.22)	0.0028 (0.10)	0.0014 (0.10)	0.0026 (0.21)	0.0028 (0.02)	0.0106 (0.06)	0.0002 (0.39)	0.0014 (0.08)	0.0019 (0.09)
β_2	0.9297 (0.00)	0.7972 (0.00)	0.9537 (0.00)	0.9357 (0.00)	0.8969 (0.00)	0.9391 (0.00)	0.9003 (0.00)	0.9016 (0.00)	0.7174 (0.00)	0.9215 (0.00)	0.9405 (0.00)	0.9046 (0.00)
β_3	0.0424 (0.21)	0.7558 (0.00)	0.0734 (0.01)	0.1573 (0.01)	0.1477 (0.01)	0.0901 (0.02)	0.1785 (0.00)	0.2220 (0.00)	0.3821 (0.00)	0.2101 (0.00)	0.0969 (0.01)	0.1876 (0.00)
β_4	0.1440 (0.02)	- 0.2136 (0.00)	0.1125 (0.00)	0.1711 (0.01)	0.1952 (0.00)	0.1020 (0.00)	0.1256 (0.03)	0.0927 (0.03)	0.4085 (0.00)	0.1415 (0.24)	0.0952 (0.05)	0.1379 (0.06)
DQ	0.88	0.58	0.51	0.20	0.99	0.69	0.75	0.54	0.70	0.90	0.58	0.79
	GERMANY	GREECE	HUNGARY	IRELAND	ITALY	NETHERLANDS	POLAND	PORUGAL	SLOVENIA	SPAIN	SLOVAKIA	UK
β_1	0.0017 (0.08)	0.0004 (0.43)	0.0052 (0.00)	0.0017 (0.25)	0.0016 (0.18)	0.0017 (0.02)	0.0013 (0.08)	-0.0024 (0.25)	0.0001 (0.35)	0.0014 (0.03)	0.0016 (0.19)	0.0013 (0.16)
β_2	0.9349 (0.00)	0.9278 (0.00)	0.8508 (0.00)	0.8015 (0.00)	0.8014 (0.00)	0.9354 (0.00)	0.9256 (0.00)	0.8605 (0.00)	0.9748 (0.00)	0.8865 (0.00)	0.9021 (0.00)	0.9599 (0.00)
β_3	0.0901 (0.01)	0.1826 (0.00)	0.2208 (0.00)	0.4397 (0.00)	0.5718 (0.00)	0.1031 (0.00)	0.1151 (0.00)	0.4621 (0.00)	0.0790 (0.00)	0.3688 (0.00)	0.2008 (0.00)	0.0389 (0.07)
β_4	0.1176 (0.01)	0.1140 (0.06)	0.2128 (0.00)	0.4085 (0.00)	0.2498 (0.17)	0.0932 (0.01)	0.1318 (0.00)	0.2358 (0.01)	0.0258 (0.08)	0.0885 (0.05)	0.1690 (0.01)	0.0775 (0.01)
DQ	0.08	0.47	0.08	0.75	0.55	0.92	0.18	0.61	0.71	0.90	0.88	0.79
	HONG KONG	JAPAN	MALAYSIA	NORWAY	NEW ZEALAND	ROMANIA	SWEDEN	SINGAPORE	TURKEY	RUSSIA	USA	VENUEZUELA
β_1	0.0004 (0.28)	0.0005 (0.05)	0.0554 (0.00)	0.0002 (0.45)	0.0106 (0.02)	0.0033 (0.20)	0.0017 (0.03)	0.0042 (0.00)	0.0082 (0.12)	0.0039 (0.00)	0.0018 (0.14)	0.2404 (0.04)
β_2	0.9357 (0.00)	0.9299 (0.00)	- 0.0764 (0.00)	0.9317 (0.00)	0.7891 (0.00)	0.8200 (0.00)	0.9425 (0.00)	0.8710 (0.00)	0.8486 (0.00)	0.8582 (0.00)	0.9129 (0.00)	0.4235 (0.07)
β_3	0.1028 (0.01)	0.2147 (0.00)	0.9976 (0.00)	0.0791 (0.01)	0.1304 (0.02)	0.4692 (0.05)	0.0308 (0.18)	0.1947 (0.00)	0.2900 (0.05)	0.2873 (0.00)	0.1596 (0.02)	0.1854 (0.09)
β_4	0.1472 (0.00)	0.0396 (0.06)	0.0320 (0.12)	0.2060 (0.00)	0.3472 (0.00)	0.3354 (0.00)	0.1366 (0.00)	0.1545 (0.00)	0.3157 (0.09)	0.2392 (0.00)	0.1321 (0.00)	0.4561 (0.06)
DQ	0.10	0.96	0.51	0.93	0.03	0.13	0.32	0.99	0.82	0.67	0.51	0.65

Note: Sovereign bonds are indicated by the corresponding country acronym. For each β we report in brackets the corresponding p -value. Parameters with a p -value smaller than 1% are reported in bold. The DQ-test is the p -value of the Dynamical Quantile test of Engle and Manganelli (2004). A value of the test below 1% means that the hypothesis that the model (16) fits the data is rejected with a confidence of 1%.

Appendix A. Time-adapted CAViAR

We first review the CAViAR estimation method introduced by Engle and Manganelli (2004). Given a time series $\{Y_t\}_{t=1}^T$ the conditional Value-at-Risk is the time series $\{V_t^{(\alpha)}\}_{t=1}^T$ implicitly defined by the equation

$$\alpha = \text{Prob} \left[Y_t < -V_t^{(\alpha)} | I_{t-1} \right]. \tag{15}$$

The quantile regression developed by Engle and Manganelli (2004) allows for the estimation of any parametric model for $V_t^{(\alpha)}$. In testing tail risk spillovers among financial time series, Hong et al. (2009) adopt the asymmetric slope model that specifies $V_t^{(\alpha)}$ as

$$V_t^{(\alpha)} = \beta_1 + \beta_2 V_{t-1}^{(\alpha)} + \beta_3 Y_{t-1}^+ + \beta_4 Y_{t-1}^-, \tag{16}$$

where the dependence of the β 's from α has been omitted to ease the notation and where the Y_{t-1}^+ (resp. Y_{t-1}^-) denotes the positive (resp. negative) part. Volatility clustering implies that a strongly positive significant β_2 is expected. Concerning β_3 and β_4 they define, respectively, the impact of positive and negative returns on future Value-at-Risk. Models such that reported in Eq. (16) are estimated in Engle and Manganelli (2004) through a quantile regression. In estimating model (16) on equity and bond returns we adopt the same procedure as well (see Section 6 of Engle and Manganelli, 2004 for more details). For our purposes, however, we have to take particular care since we are aimed at producing fully-causal time series of conditional Value-at-Risk of equity and bonds. Hence we have to fix two main issues. First, we want to have time series that are comparable with each other and then we have to

mitigate the asynchronicity due to the different time zones of the countries in our dataset. Second, having in mind a Granger-type analysis, at each point in time only past information should be used to produce the Value-at-Risk estimates.

We start our procedure with a “training” window of six years. More precisely, to compute the initial value of the VaR time series, we use a window starting in $t_{\text{start}} = \text{January, 1, 2001}$ and ending at $t_{\text{end}}^{(0)} = \text{January, 1, 2006}$.²⁰ Then, for a given series either of equity log-returns or of bond yield variations, we estimate the model of Eq. (16). Hence, the final date $t_{\text{end}}^{(0)}$ is shifted by one month producing a new final date $t_{\text{end}}^{(1)} = t_{\text{end}}^{(0)} + 1 \text{ month}$ and the estimation procedure, now using data from t_{start} up to $t_{\text{end}}^{(1)}$ is repeated. The generic n th time window is thus formed using data from t_{start} up to $t_{\text{end}}^{(n)} \equiv t_{\text{end}}^{(0)} + n \text{ months}$. The procedure is iterated over n until the end of the time stamp is reached, that is when the shifted final date $t_{\text{end}}^{(n)}$ occurs after February, 14, 2014, which is the last available day for all time series in the dataset.

The outcome of the procedure is the set of $Z_{i,t}^B = \mathbb{1} \left\{ Y_{i,t} < -V_{i,t}^{(\alpha)} \left(\hat{\vartheta}_i \right) \right\}$ series where t spans across the 2-days time grid, $Y_{i,t}$ is either the series of bond yield variations or the

²⁰ This choice does not affect country whose series is not available before January, 1, 2006. In fact, before proceeding to the estimation of the CAViAR model, we require that at least 100 (daily) observations of the series are present. This limitation is required since we initialize the CAViAR estimation with the first 10% of the series, hence a reasonable number of observations must be present in order to have a reliable estimate of $V_0^{(\alpha)}$ in (16).

Table 3
Parameter estimates of the model (16) for the daily time series of equity log-returns of the 33 systemically important financial institutions.

	Equity Ticker											
	DEXB	CS	UBS	CBK	DB	SAN	BBVA	ACA	GLE	BNP	RBS	
β_1	0.0043 (0.03)	0.0010 (0.00)	0.0006 (0.02)	0.0015 (0.01)	0.0014 (0.02)	0.0006 (0.02)	0.0014 (0.00)	0.0005 (0.02)	0.0011 (0.00)	0.0009 (0.00)	0.0008 (0.01)	
β_2	0.7899 (0.00)	0.9032 (0.00)	0.9264 (0.00)	0.8597 (0.00)	0.8689 (0.00)	0.9290 (0.00)	0.8666 (0.00)	0.9429 (0.00)	0.9102 (0.00)	0.9083 (0.00)	0.9302 (0.00)	
β_3	0.1022 (0.00)	0.0806 (0.05)	0.0412 (0.29)	0.1245 (0.04)	0.1011 (0.00)	0.0054 (0.42)	0.1179 (0.00)	0.0419 (0.17)	0.0460 (0.15)	0.0435 (0.17)	0.0344 (0.21)	
β_4	0.4882 (0.00)	0.2532 (0.00)	0.2132 (0.00)	0.3574 (0.00)	0.3807 (0.00)	0.2421 (0.00)	0.3275 (0.00)	0.1576 (0.00)	0.2658 (0.00)	0.2760 (0.00)	0.2037 (0.00)	
DQ	0.64	0.96	0.79	0.80	0.50	0.63	0.83	0.60	0.84	0.58	0.67	
	STAN	HSBC	LLOY	BCS	UCG	NDA	RF	COF	GS	JPM	AXP	
β_1	0.0005 (0.05)	0.0007 (0.04)	0.0004 (0.00)	0.0005 (0.20)	0.0009 (0.01)	0.0013 (0.06)	0.0002 (0.25)	0.0009 (0.00)	0.0008 (0.01)	0.0007 (0.12)	0.0005 (0.06)	
β_2	0.8889 (0.00)	0.8446 (0.00)	0.9483 (0.00)	0.9335 (0.00)	0.9213 (0.00)	0.8503 (0.00)	0.9182 (0.00)	0.9011 (0.00)	0.8868 (0.00)	0.9197 (0.00)	0.8934 (0.00)	
β_3	0.1079 (0.15)	0.1907 (0.00)	−0.0315 (0.04)	0.0202 (0.34)	0.0456 (0.21)	0.1703 (0.07)	0.0938 (0.10)	0.0512 (0.13)	0.1250 (0.00)	0.0933 (0.12)	0.1225 (0.00)	
β_4	0.2857 (0.01)	0.4594 (0.00)	0.2205 (0.00)	0.2228 (0.00)	0.2109 (0.02)	0.3449 (0.00)	0.2214 (0.02)	0.2732 (0.00)	0.2981 (0.05)	0.1627 (0.02)	0.2832 (0.00)	
DQ	0.91	0.94	0.57	0.26	0.37	0.95	0.75	0.93	0.75	0.56	0.64	
	BBT	BAC	BK	C	FITB	MS	PNC	STT	STI	USB	WFC	
β_1	0.0003 (0.17)	0.0015 (0.07)	0.0008 (0.03)	0.0009 (0.00)	0.0005 (0.11)	0.0008 (0.00)	0.0001 (0.42)	0.0012 (0.00)	0.0004 (0.11)	0.0001 (0.42)	−0.0000 (0.50)	
β_2	0.9034 (0.00)	0.8398 (0.00)	0.9158 (0.00)	0.9072 (0.00)	0.9498 (0.00)	0.8991 (0.00)	0.9068 (0.00)	0.8554 (0.00)	0.9100 (0.00)	0.8396 (0.00)	0.9086 (0.00)	
β_3	0.1074 (0.01)	0.1337 (0.03)	0.0558 (0.05)	0.0483 (0.19)	0.0055 (0.44)	0.0588 (0.05)	0.0718 (0.24)	0.0979 (0.17)	0.0557 (0.28)	0.1839 (0.00)	0.1065 (0.00)	
β_4	0.3119 (0.00)	0.4188 (0.08)	0.2209 (0.00)	0.2843 (0.00)	0.1541 (0.00)	0.3133 (0.00)	0.3566 (0.00)	0.3985 (0.00)	0.2872 (0.00)	0.5056 (0.00)	0.2978 (0.00)	
DQ	0.23	0.70	0.61	0.15	0.96	0.86	0.71	0.66	0.87	0.93	0.22	

Note: Equities are indicated by the corresponding ticker. For each β we report in brackets the corresponding p -value. Parameters with a p -value smaller than 1% are reported in bold. The DQ-test is the p -value of the Dynamical Quantile test of Engle and Manganelli (2004). A value of the test below 1% means that the hypothesis that the model (16) fits the data is rejected with a confidence of 1%.

series of equity log-returns, $V_{i,t}^{(\alpha)}(\hat{\beta}_i)$ is the series of the estimated

Value-at-Risk of $Y_{i,t}$, and $\hat{\beta}_i = \{\beta_i, i = 1, \dots, 4\}$ is the parameter vector. We stress that, as mentioned in Section 4, while all the information available up to $t_{\text{end}}^{(n)}$ is used to estimate the parametric model (16), all networks of Granger causalities are formed only with data in the three years prior to $t_{\text{end}}^{(n)}$, where the choice of three years is a trade-off between the power of the causality tests and the necessity of isolating periods of financial distress.

In Tables 2 and 3 we report the estimated β 's and the corresponding p -value (in brackets) for, respectively, the 36 sovereign debt bonds and the 33 systemically important financial institutions in our dataset, estimated using the entire time span. Numbers in bold identify 99% significant parameters. The adequacy of the fit is measured by the p -value of the dynamical quantile (DQ) test of Engle and Manganelli (2004) reported in Tables 2 and 3 for each time series.²¹

Appendix B. Summary statistics

This Appendix reports the summary statistics of the three blocks of data as introduced in Section 3.

Table 4 shows a summary statistics of the series of bond yield variations used for the construction of the causal network. Moreover, for each country we add the information coming from

²¹ A p -value below 0.01 means that the hypothesis that model (16) is the true DGP is rejected with 99% confidence.

historical S&P long-term foreign currency ratings that is explicitly used in the flight-to-quality analysis of Section 5.

Similarly, Table 5 reports a summary statistics for the time series of equity log-returns, which, typically, are available for longer time periods. As for the bond series, all equity series end at February, 14, 2014. Note that in both Tables 4 and 5 the number of observations refers to the number of bond yield variations or equity log-returns in a two-days sub-sampled grid, and thus it is typically half of what it is expected from a daily time series. As anticipated in the main text, the sub-sampling is required in order to mitigate the effect of non-synchronous data (equities and bonds may refer to banks or countries that pertain to different parts of the world).

A third block of data is formed by CDS spreads. This part of the dataset is extensively adopted in Section 6.1 to define quality measures that are suitable for the proposed out-of-sample forecast exercise and that are (at least by construction) independent from the S&P country ratings. Table 6 reports a summary statistics for the CDS spread dataset. It is worth to mention that, despite all bond and equity series end at February, 14, 2014 (even if the starting date may vary from series to series), all CDS spread series end mostly at January, 13, 2014, with few exceptions. Moreover, while the summaries for bonds and equities in Tables 4 and 5 are related to one-lag differences (or log-differences) on a two-days subsampled grid, the summary for CDS spread is relative to the original daily grid. This is because, for a given country, the corresponding CDS spreads are used in Section 6.1 for the construction of a measure of bond quality in connection with the bond yield of the same country, hence there are no issues related to non-synchronicity of data. In this case we also rely on the original daily grid for bond yields as well.

Table 4
Summary statistics for five-years maturity sovereign bond yield variations.

Country	#Obs	First Yield	First Rating	Mean	Std	Kurt	Skew	Rat. Initial	Rat. Final
Australia	1707	18-Dec-2000	30-Apr-2003	-0.0011614	0.086692	4.1985	0.10344	AAA	AAA
Bulgaria	918	17-Jan-2007	28-Feb-2001	-0.0021423	0.26788	11.4813	-0.025379	BB	BBB
Canada	1563	06-Feb-2002	01-Jan-2003	-0.0018417	0.070579	5.061	0.15631	AAA	AAA
Switzerland	912	05-Feb-2007	05-Jun-2007	-0.0025198	0.048724	11.7672	-0.97995	AAA	AAA
Czech Rep.	1707	22-Dec-2000	26-Feb-2001	-0.0032534	0.072267	13.8517	-0.12909	AA	AA
Denmark	1707	18-Dec-2000	26-Nov-2002	-0.0024144	0.066528	4.6618	0.19488	AAA	AAA
Austria	1707	18-Dec-2000	29-May-2001	-0.0022451	0.069703	8.0128	0.14315	AAA	AA
Belgium	1707	18-Dec-2000	31-Jan-2001	-0.0021455	0.079765	17.4321	-0.28795	AA	AA
Croatia	1707	23-Feb-1999	04-Jan-2001	-0.0013913	0.073417	12.5473	0.81739	A	BBB
Cyprus	1248	08-Jul-2004	01-Feb-2002	0.00288	0.2969	87.3243	2.2977	A	BB
Finland	1044	31-Jan-2006	23-Apr-2001	-0.0022283	0.068877	4.6478	-0.0046261	AAA	AAA
France	1044	31-Jan-2006	12-Apr-2002	-0.002152	0.072982	6.0037	-0.17405	AAA	AA
Germany	1707	21-Dec-2000	02-Jul-2002	-0.0022529	0.068445	4.661	0.09215	AAA	AAA
Greece	1249	05-Jul-2004	02-Jan-2001	-0.0019649	0.87615	20.659	0.86456	AA	CC
Hungary	1707	26-Jan-1999	28-Feb-2001	-0.00073451	0.12418	127.6168	7.0949	A	BB
Ireland	1707	12-Jan-1999	01-Jan-2003	-0.0016136	0.14665	37.0698	-1.4267	AA	BBB
Italy	1050	12-Jan-2006	31-Jan-2001	-0.00060661	0.13384	17.3076	-0.59019	AA	BBB
Netherlands	1707	19-Dec-2000	31-Jul-2003	-0.0021168	0.066599	4.6625	0.13765	AAA	AAA
Poland	1437	27-Jan-2003	04-Jan-2001	-0.0016577	0.071337	26.6904	2.2572	BBB	A
Portugal	899	13-Mar-2007	07-Feb-2002	2.3583e-05	0.31568	25.2	0.29047	AA	BB
Slovenia	1707	22-Dec-2000	26-Apr-2001	-0.00095375	0.095164	46.5957	3.0981	A	A
Spain	1707	21-Dec-2000	31-Jan-2001	-0.0014353	0.11052	17.1361	-1.0718	AA	BBB
Slovakia	1260	04-Jun-2004	24-May-2001	-0.0026884	0.071821	12.7855	0.29499	BBB	A
United Kingdom	1707	21-Dec-2000	27-Oct-2004	-0.001923	0.068336	5.2821	-0.00094986	AAA	AAA
Hong Kong	1036	22-Feb-2006	02-Jul-2002	-0.0026838	0.070906	6.4891	0.33106	A	AAA
Japan	1707	21-Dec-2000	04-Jan-2001	-0.00044238	0.034059	8.13	0.5942	AA	AA
Malaysia	885	19-Apr-2007	23-Apr-2001	0.00050054	0.099712	245.6309	-0.70101	BBB	A
Norway	1707	27-Dec-2000	24-Oct-2003	-0.0021842	0.074505	7.0371	0.06374	AAA	AAA
New Zealand	892	02-Apr-2007	31-Jul-2003	-0.0025713	0.070055	5.8272	0.10122	AA	AA
Romania	912	02-Feb-2007	11-Feb-2002	-0.0024293	0.22238	39.5595	0.066911	B	BB
Sweden	1201	17-Nov-2004	04-Jan-2001	-0.001455	0.065942	6.4749	-0.35297	AA	AAA
Singapore	943	08-Nov-2006	18-Jul-2003	-0.0016856	0.061072	10.2324	0.57176	AAA	AAA
Turkey	1209	25-Oct-2004	19-Jan-2001	-0.007365	0.46916	84.4745	2.0867	B	BB
Russia	1707	03-Jan-2000	23-Apr-2001	-0.0076673	0.15226	23.197	0.51217	BB	BBB
United States	1153	31-Mar-2005	01-Dec-2003	-0.0023223	0.089286	5.4863	0.21661	AAA	AA
Venezuela	668	17-Dec-2008	26-Feb-2001	-0.0071942	0.33779	5.7275	0.13542	B	B

Note: Summary statistics for the bond sample. The first column is the name of the country. The second column indicates the total number of available observations, that is the total number of innovations (one-lag differences of bond yields) in the two-days sub-sampled grid. Despite the starting date may vary from series to series, the ending date is February, 14, 2014 for all the countries. The third column is the starting date of the series, that is when the first yield is available. The fourth column indicates when the first S&P rating is available. Mean, Std, Kurt and Skew indicate, respectively, mean, standard deviation, kurtosis and skewness of the corresponding series for the entire sample. Finally, the last two columns indicate, respectively, the initial and final S&P rating.

Appendix C. Granger causality

Billio et al. (2012) apply the definition of causality as originally defined by Granger (1969). Consider two time series $\{Y_{1,t}\}_{t=1}^T$ and $\{Y_{2,t}\}_{t=1}^T$ and the two regressions

$$Y_{1,t+1} = b_{1,1} Y_{1,t} + \varepsilon_{t+1} \tag{17}$$

$$Y_{1,t+1} = b_{1,1} Y_{1,t} + b_{1,2} Y_{2,t} + \psi_{t+1},$$

where ε_{t+1} and ψ_{t+1} are i.i.d. normal shocks (with possibly non-zero mean). When testing the Granger (1969)-causality we are testing the null

$$\mathbb{H}_G^0 : \mathbb{E} \left[Y_{1,t} | \{Y_{1,t-k}\}_{k=1}^{t-1} \right] = \mathbb{E} \left[Y_{1,t} | \{Y_{1,t-k}, Y_{2,t-k}\}_{k=1}^{t-1} \right] \tag{18}$$

against the alternative

$$\mathbb{H}_G^A : \mathbb{E} \left[Y_{1,t} | \{Y_{1,t-k}\}_{k=1}^{t-1} \right] \neq \mathbb{E} \left[Y_{1,t} | \{Y_{1,t-k}, Y_{2,t-k}\}_{k=1}^{t-1} \right]. \tag{19}$$

We say that $\{Y_{2,t}\}_{t=1}^T$ Granger-causes the series $\{Y_{1,t}\}_{t=1}^T$, and we write $(2 \Rightarrow 1)$, at a confidence level α if the F-statistic of the two regressions

$$F = \left(\sum_{t=1}^T (\hat{\varepsilon}_t^2 - \hat{\psi}_t^2) \right) \left(\frac{\sum_{t=1}^T \hat{\psi}_t^2}{T-2} \right)^{-1}$$

is larger than the corresponding α -quantile of the F-distribution. Note that with this definition we are not testing for simultaneous causality. This choice is necessary in order to have a coherent comparison with the $Q_1(M)$ test, which does not check for simultaneous risk spillover.

In order to avoid spurious detections (induced by heteroskedasticity) of causalities in the Granger (1969)-causality network we follow the procedure adopted by Billio et al. (2012) and we filter out a GARCH(1, 1) model from data. That is, for each time series $Y_{i,t}$, we estimate the model

$$\begin{cases} Y_{i,t} = \mu_i + \sigma_{i,t} \varepsilon_{i,t}, \varepsilon_{i,t} \sim N(0, 1), \\ \sigma_{i,t}^2 = \omega_i + \alpha_i (Y_{i,t-1} - \mu_i)^2 + \beta_i \sigma_{i,t-1}^2, \end{cases} \tag{20}$$

and then normalize each time series by re-defining

$$Y_{i,t} \equiv \frac{Y_{i,t}}{\hat{\sigma}_{i,t}}$$

where $\hat{\sigma}_{i,t}$ is the estimated conditional volatility of model (20). This filtering is not required for the tail risk networks since heteroskedasticity is, in these cases, taken into account by the parametric conditional Value-at-Risk model.

Table 5
Summary statistics for equity log-returns.

Ticker	#Obs	First Price	Mean	Std	Kurt	Skew
DEXB	1707	07-Oct-1999	-0.0035184	0.072745	15.2732	0.079262
CS	1643	27-Jun-2001	-0.00048936	0.038509	11.2898	0.32927
UBS	1681	14-Mar-2001	-0.00043545	0.03446	11.2177	-0.079069
CBK	1707	22-Apr-1998	-0.00054483	0.03749	10.5217	-0.052093
DB	1707	22-Apr-1998	-0.0015446	0.044453	10.2787	-0.41609
SAN	1707	22-Apr-1998	-0.00033222	0.031501	6.3791	0.062805
BBVA	1707	29-Dec-1999	-0.00034258	0.032301	6.446	-0.023647
ACA	1602	22-Oct-2001	-0.00035503	0.038336	8.253	-0.09679
GLE	1707	22-Oct-1998	-0.0002281	0.041138	7.6145	-0.1066
BNP	1707	22-Oct-1998	0.00017214	0.036591	8.1942	0.050653
RBS	1707	24-Mar-1999	0.00016734	0.032294	11.1185	-0.17534
STAN	1707	04-Feb-1999	-0.00021892	0.025165	16.1126	-0.86996
HSBC	1707	02-Feb-1999	-0.0010079	0.046532	24.338	-1.4578
LLOY	1707	02-Feb-1999	-0.00033476	0.046943	26.2879	0.26912
BCS	1707	10-Dec-1998	-0.0015173	0.053786	163.7187	-7.4101
UCG	1707	19-Aug-1998	-0.00099158	0.036409	9.1553	-0.11276
NDA	1707	22-Jun-1998	0.00038478	0.02919	8.9226	0.15603
RF	1707	14-Dec-1998	0.00034582	0.032113	13.4261	0.07461
COF	1707	26-Apr-1999	-1.6519e-06	0.029675	16.539	0.56877
GS	1707	14-Dec-1998	-0.00019598	0.042239	21.9987	-0.21996
JPM	1122	27-Jun-2005	4.1355e-05	0.030608	11.4117	-0.38165
AXP	1707	27-Apr-1999	6.3366e-05	0.043883	16.9162	-0.50853
BBT	1707	14-Dec-1998	-0.0013513	0.045729	21.7681	-0.57551
BAC	1707	18-Jun-1999	-0.00061847	0.052349	69.6301	2.3045
BK	1707	15-Jun-1999	0.00025387	0.032615	10.7813	-0.1228
C	1707	10-May-2000	0.00010819	0.033869	10.7917	-0.082293
FITB	1707	15-Dec-1998	-0.00042313	0.053264	70.7717	1.4406
MS	1707	16-Jun-1999	5.7451e-05	0.035257	36.7378	-1.5176
PNC	1187	27-Dec-2004	-0.0010434	0.052744	16.4883	0.27674
STT	1707	18-Jun-1999	7.2277e-05	0.039327	58.6034	-2.9936
STI	1707	23-Oct-1998	-0.00031073	0.041151	34.4266	1.1071
USB	1707	18-Jun-1999	0.00017	0.032021	26.1179	-0.4025
WFC	1707	14-Dec-1998	0.00029344	0.03257	20.9868	-0.35808

Note: Summary statistics for the equity sample. The first column indicates the bank ticker. The second column indicates the total number of available observations, that is the total number of innovations (one-lag differences of equity log-prices) in the two-days sub-sampled grid. Despite the starting date may vary from series to series, the ending date is February, 14, 2014 for all the equities. The third column is the starting date of the series, that is when the first price is available. Mean, Std, Kurt and Skew indicate, respectively, mean, standard deviation, kurtosis and skewness of the corresponding equity for the entire sample.

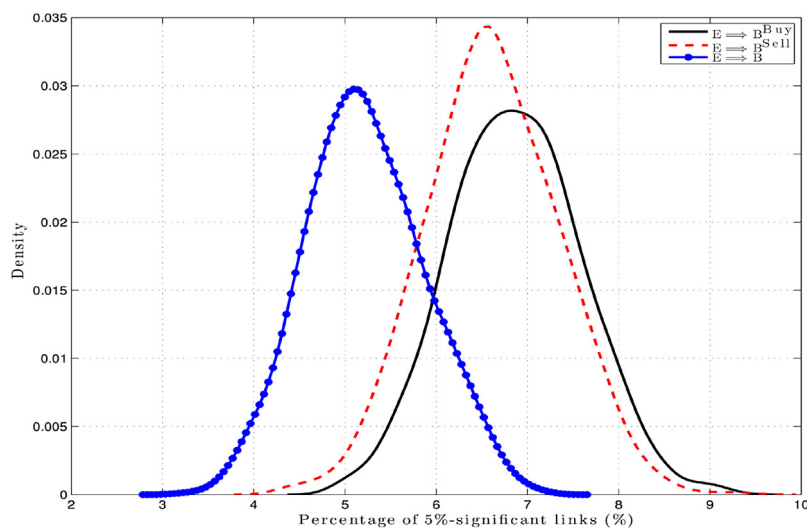


Fig. 11. The black (continuous), the red (dotted) and the blue (with filled circles) lines represent, respectively, the density of the percentage of 5%-significant links according to the $(E_j \Rightarrow B_i^{\text{Buy}})$, $(E_j \Rightarrow B_i^{\text{Sell}})$ and $(E_j \Rightarrow B_i)$ causality test. The density is computed over 1000 replications of a bootstrap procedure in which, for each replication, a new set of 33 equity log-returns and 36 bond yield variations is formed by randomly extracting with replacement 400 observations from the original time series. Densities are normalized to have an integral equal to one. (For interpretation of the references to color in this legend, the reader is referred to the web version of the article.)

Appendix D. Monte Carlo estimation of the confidence intervals of the centrality measures

Figs. 1 and 3 report the percentage of 5%-significant links in the bi-partite network of equity-bond, estimated in a rolling time-window of three years. In the ideal case in which the network is

estimated via an infinite time series, both the causal test and the estimation of the VaR model in (16) or the GARCH model in (20) are immune by estimation errors. In this case we expect 5% of the equity-bond couples to be validated under the null of no-causal connections among them. In practice, finiteness of the sample and numerical errors in the estimation procedure could result in higher

Table 6
Summary statistics for five-years maturity CDS spread variations.

Country	#Obs	First Obs.	Last Obs.	Mean	Std	Kurt	Skew
Australia	2697	30-Apr-2003	13-Jan-2014	8.4894e-07	0.00021067	26.3281	0.51716
Bulgaria	3342	28-Feb-2001	13-Jan-2014	-1.1356e-05	0.00088362	99.5856	-2.9087
Canada	2283	11-Sep-2003	13-Jan-2014	-1.3333e-06	0.00013204	34.555	-1.851
Switzerland	1308	05-Jun-2007	13-Jan-2014	-1.9349e-06	0.00025046	41.9152	-0.89803
Czech Rep.	3251	26-Mar-2001	13-Jan-2014	1.0436e-06	0.00034909	51.6964	0.45145
Denmark	2877	26-Nov-2002	13-Jan-2014	5.9399e-07	0.00018683	27.1692	0.44277
Austria	3295	29-May-2001	13-Jan-2014	9.8893e-07	0.00030032	37.8286	1.136
Belgium	3374	31-Jan-2001	13-Jan-2014	1.1869e-06	0.00038992	38.4293	-0.79271
Croatia	3398	04-Jan-2001	13-Jan-2014	1.792e-06	0.0007084	30.0985	-0.52374
Cyprus	2785	01-Jul-2002	13-Jan-2014	2.663e-05	0.0016567	99.2018	1.4096
Finland	2983	01-Jul-2002	13-Jan-2014	5.1689e-07	0.00011401	22.0623	0.92094
France	3061	12-Apr-2002	13-Jan-2014	1.5933e-06	0.00026709	23.924	-0.26315
Germany	2946	02-Jul-2002	13-Jan-2014	6.9075e-07	0.00014363	19.351	0.225
Greece	3036	02-Jan-2001	13-Jan-2014	0.00074927	0.02616	547.4371	13.5898
Hungary	2816	28-Feb-2001	29-Dec-2011	2.0483e-05	0.00083989	47.3315	1.7824
Ireland	2878	01-Jan-2003	13-Jan-2014	3.623e-06	0.0010063	45.6246	-0.62625
Italy	3379	31-Jan-2001	13-Jan-2014	4.3708e-06	0.0006985	26.7496	0.12638
Netherlands	2316	31-Jul-2003	13-Jan-2014	1.0806e-06	0.00019783	25.9883	1.0971
Poland	3372	04-Jan-2001	13-Jan-2014	1.0346e-06	0.00049855	35.175	0.12573
Portugal	3113	07-Feb-2002	13-Jan-2014	8.9085e-06	0.0014123	39.4631	-0.44806
Slovenia	3106	01-Feb-2002	13-Jan-2014	5.5031e-06	0.0004897	47.888	2.0997
Spain	3361	26-Feb-2001	13-Jan-2014	3.7635e-06	0.00070193	21.9508	-0.57469
Slovakia	3277	24-May-2001	13-Jan-2014	-1.9518e-06	0.00035572	31.4529	1.2219
United Kingdom	1991	20-Mar-2006	13-Jan-2014	1.2377e-06	0.00021594	15.3519	-0.2338
Hong Kong	2479	29-Aug-2003	13-Jan-2014	1.1084e-06	0.00029628	65.5134	3.1484
Japan	3380	04-Jan-2001	13-Jan-2014	9.6021e-07	0.00019432	59.3879	2.3455
Malaysia	3321	23-Apr-2001	13-Jan-2014	-1.3894e-06	0.00056761	159.714	1.0161
Norway	2657	24-Oct-2003	13-Jan-2014	4.1095e-07	0.00011122	47.1808	0.64787
New Zealand	2429	31-Jul-2003	13-Jan-2014	1.7824e-06	0.00028063	36.5511	0.46946
Romania	3051	21-Mar-2002	13-Jan-2014	-1.1689e-05	0.0010779	96.6887	-2.8478
Sweden	3008	29-May-2001	13-Jan-2014	3.2633e-07	0.00015686	31.691	0.50626
Singapore	1896	18-Jul-2003	23-Mar-2012	4.8426e-06	0.00016737	547.7068	17.8006
Turkey	3387	19-Jan-2001	13-Jan-2014	-8.7661e-06	0.0014769	72.3195	3.6072
Russia	3215	18-Sep-2001	13-Jan-2014	-1.8761e-05	0.0012738	88.5448	2.6698
United States	2581	01-Dec-2003	13-Jan-2014	1.0715e-06	0.00012687	20.2746	0.79051
Venezuela	3361	26-Feb-2001	13-Jan-2014	1.5273e-05	0.003007	57.8959	0.54851

Note: Summary statistics for the CDS spread sample. The first column is the name of the country. The second column indicates the total number of available observations, that is the total number of CDS spreads (one-lag differences) sampled at daily frequency. The third column is the starting date of the series, that is when the first CDS spread is available. The fourth column indicates when the series ends. Note that, differently from the bond yield and equity series, not all CDS series end at the same date, this is why the termination date is reported here for CDS spreads but omitted in Tables 4 and 5. Mean, Std, Kurt and Skew indicate, respectively, mean, standard deviation, kurtosis and skewness of the corresponding series for the entire sample.

rejection rates under the null. In order to validate the statistical significance of the results shown in Figs. 1 and 3 we perform a simple Monte Carlo experiment. For each equity and bond series in the dataset we randomly extract with replacement 400 observations from the corresponding time-series, hence forming a new set of 33 equity log-returns and 36 bond yield variations. The choice of 400 observations is dictated by the need of reproducing the sample size used for the estimation of the causal networks. After a new set of bootstrapped equity-bond data is formed, we proceed in the estimation of the three casual networks and we record the percentage of validated links at 5% confidence level. We iterate this procedure for 1000 times and we plot in Fig. 11 the density plots of the three percentages of validated links, one for each type of causality. The horizontal lines in Figs. 1 and 3 are in correspondence of the average percentage of 5%-validated links computed over the 1000 replications. These values are 6.8%, 6.6% and 5.2% for, respectively, the $(E_j \Rightarrow B_i^{\text{Buy}})$, $(E_j \Rightarrow B_i^{\text{Sell}})$ and $(E_j \Rightarrow B_i)$ causal networks. The slightly larger values found for the networks of tail causality is mainly a consequence of the unavoidable smaller statistic of the tail events.

References

- Adrian, T., Brunnermeier, M.K., 2016. CoVaR. *Am. Econ. Rev.* 106 (7), 1705–1741.
 Adrian, T., Shin, H.S., 2010. Liquidity and leverage. *J. Financ. Intermed.* 19 (3), 418–437.
 Adrian, T., Shin, H.S., 2014. Procyclical leverage and value-at-risk. *Rev. Financ. Stud.* 27 (2), 373–403.
 Allen, L., Bali, T.G., Tang, Y., 2012. Does systemic risk in the financial sector predict future economic downturns? *Rev. Financ. Stud.* 25 (10), 3000–3036.
 Anderson, R.G., Liu, Y., 2013. How Low Can You Go? Negative Interest Rates and Investors' Flight to Safety. *The Regional Economist*, Federal Reserve Bank of St. Louis, pp. 12–13.
 Arnold, B., Borio, C., Ellis, L., Moshirian, F., 2012. Systemic risk, macroprudential policy frameworks, monitoring financial systems and the evolution of capital adequacy. *J. Bank. Finance* 36 (12), 3125–3132.
 Barrell, R., Davis, E.P., Karim, D., Liadze, I., 2010. Bank regulation, property prices and early warning systems for banking crises in OECD countries. *J. Bank. Finance* 34 (9), 2255–2264.
 Baur, D.G., Lucey, B.M., 2009. Flights and contagion – an empirical analysis of stock-bond correlations. *J. Financ. Stab.* 5 (4), 339–352.
 Beber, A., Brandt, M.W., Kavajecz, K.A., 2009. Flight-to-quality or flight-to-liquidity? Evidence from the euro-area bond market. *Rev. Financ. Stud.* 22 (3), 925–957.
 Billio, M., Getmansky, M., Lo, A.W., Pelizzon, L., 2012. Econometric measures of connectedness and systemic risk in the finance and insurance sectors. *J. Financ. Econ.* 104 (3), 535–559.
 Bisias, D., Flood, M., Lo, A.W., Valavanis, S., 2012. A survey of systemic risk analytics. *Annu. Rev. Financ. Econ.* 4 (1), 255–296.
 Braouezec, Y., Wagalath, L., 2018. Risk-based capital requirements and optimal liquidation in a stress scenario. *Rev. Finance* 22 (2), 747–782.
 Brownlees, C., Engle, R.F., 2016. SRISK: a conditional capital shortfall measure of systemic risk. *Rev. Financ. Stud.* 30 (1), 48–79.
 Caballero, R.J., Krishnamurthy, A., 2008. Collective risk management in a flight to quality episode. *J. Finance* 63 (5), 2195–2230.
 Chen, R.-R., Chidambaram, N., Imerman, M.B., Sopranzetti, B.J., 2014. Liquidity, leverage, and Lehman: a structural analysis of financial institutions in crisis. *J. Bank. Finance* 45, 117–139.
 Cifuentes, R., Ferrucci, G., Shin, H.S., 2005. Liquidity risk and contagion. *J. Eur. Econ. Assoc.* 3 (2–3), 556–566.
 Cont, R., Schaanning, E., 2017. Fire Sales, Indirect Contagion and Systemic Stress Testing. Working Paper 2/2017. Norges Bank, Oslo.

- Cont, R., Wagalath, L., 2013. Running for the exit: distressed selling and endogenous correlation in financial markets. *Math. Finance* 23 (4), 718–741.
- Cont, R., Wagalath, L., 2016. Fire sales forensics: measuring endogenous risk. *Math. Finance* 26 (4), 835–866.
- Corsi, F., Marmi, S., Lillo, F., 2016. When micro prudence increases macro risk: the destabilizing effects of financial innovation, leverage, and diversification. *Oper. Res.* 64 (5), 1073–1088.
- De Santis, R.A., 2014. The euro area sovereign debt crisis: identifying flight-to-liquidity and the spillover mechanisms. *J. Empir. Finance* 26, 150–170.
- Demirgüç-Kunt, A., Detragiache, E., 1998. The determinants of banking crises in developing and developed countries. *Staff Pap. Int. Monet. Fund* 45 (1), 81–109.
- Dovern, J., van Roye, B., 2014. International transmission and business-cycle effects of financial stress. *J. Financ. Stab.* 13, 1–17.
- Dutttagupta, R., Cashin, P., 2011. Anatomy of banking crises in developing and emerging market countries. *J. Int. Money Finance* 30 (2), 354–376.
- Engle, R.F., Manganelli, S., 2004. CAViaR: conditional autoregressive value at risk by regression quantiles. *J. Bus. Econ. Stat.* 22 (4), 367–381.
- Favero, C.A., 2013. Modelling and forecasting government bond spreads in the euro area: a GVAR model. *J. Econom.* 177 (2), 343–356.
- Fontana, A., Scheicher, M., 2016. An analysis of euro area sovereign CDS and their relation with government bonds. *J. Bank. Finance* 62, 126–140.
- Gârleanu, N., Pedersen, L.H., 2011. Margin-based asset pricing and deviations from the law of one price. *Rev. Financ. Stud.* 24 (6), 1980–2022.
- Geyer, A., Kossmeier, S., Pichler, S., 2004. Measuring systematic risk in EMU government yield spreads. *Rev. Finance* 8 (2), 171–197.
- Granger, C.W.J., 1969. Investigating causal relations by econometric models and cross-spectral methods. *Econometrica* 37 (3), 424–438.
- Greenwood, R., Landier, A., Thesmar, D., 2015. Vulnerable banks. *J. Financ. Econ.* 115 (3), 471–485.
- Harrington, S.E., 2009. The financial crisis, systemic risk, and the future of insurance regulation. *J. Risk Insur.* 76 (4), 785–819.
- Hong, Y., Liu, Y., Wang, S., 2009. Granger causality in risk and detection of extreme risk spillover between financial markets. *J. Econom.* 150 (2), 271–287.
- Hull, J., Predescu, M., White, A., 2004. The relationship between credit default swap spreads, bond yields, and credit rating announcements. *J. Bank. Finance* 28 (11), 2789–2811, Recent Research on Credit Ratings.
- Kaminsky, G.L., Reinhart, C.M., 1999. The twin crises: the causes of banking and balance-of-payments problems. *Am. Econ. Rev.* 89 (3), 473–500.
- Kritzman, M., Li, Y., Page, S., Rigobon, R., 2011. Principal components as a measure of systemic risk. *J. Portf. Manag.* 37 (4), 112–126.
- Manganelli, S., Wolswijk, G., 2009. What drives spreads in the euro area government bond market? *Econ. Policy* 24 (58), 191–240.
- Merton, R.C., Billio, M., Getmansky, M., Gray, D., Lo, A., Pelizzon, L., 2013. On a new approach for analyzing and managing macrofinancial risks. *Financ. Anal. J.* 69 (2), 22–33.
- Oet, M.V., Bianco, T., Gramlich, D., Ong, S.J., 2013. SAFE: an early warning system for systemic banking risk. *J. Bank. Finance* 37 (11), 4510–4533.
- Pesaran, M.H., Schuermann, T., Smith, L.V., 2009. Forecasting economic and financial variables with global VARs. *Int. J. Forecast.* 25 (4), 642–675.
- Petrella, G., Resti, A., 2017. What drives the liquidity of sovereign bonds when markets are under stress? An assessment of the new Basel 3 rules on bank liquid assets. *J. Financ. Stab.* 33, 297–310.
- Scheffer, M., Bascompte, J., Brock, W.A., Brovkin, V., Carpenter, S.R., Dakos, V., Held, H., van Nes, E.H., Rietkerk, M., Sugihara, G., 2009. Early-warning signals for critical transitions. *Nature* 461 (7260), 53–59.
- Scheffer, M., Carpenter, S.R., Lenton, T.M., Bascompte, J., Brock, W., Dakos, V., van de Koppel, J., van de Leemput, I.A., Levin, S.A., van Nes, E.H., Pascual, M., Vandermeer, J., 2012. Anticipating critical transitions. *Science* 338 (6105), 344–348.
- Vuong, Q.H., 1989. Likelihood ratio tests for model selection and non-nested hypotheses. *Econometrica* 57 (2), 307–333.